Master Thesis in Geosciences

Reservoir Quality in the Jurassic sandstones reservoirs located in the Central Graben

A sedimentological and petrophysical approach

Ali Mustafa Khan Niazi

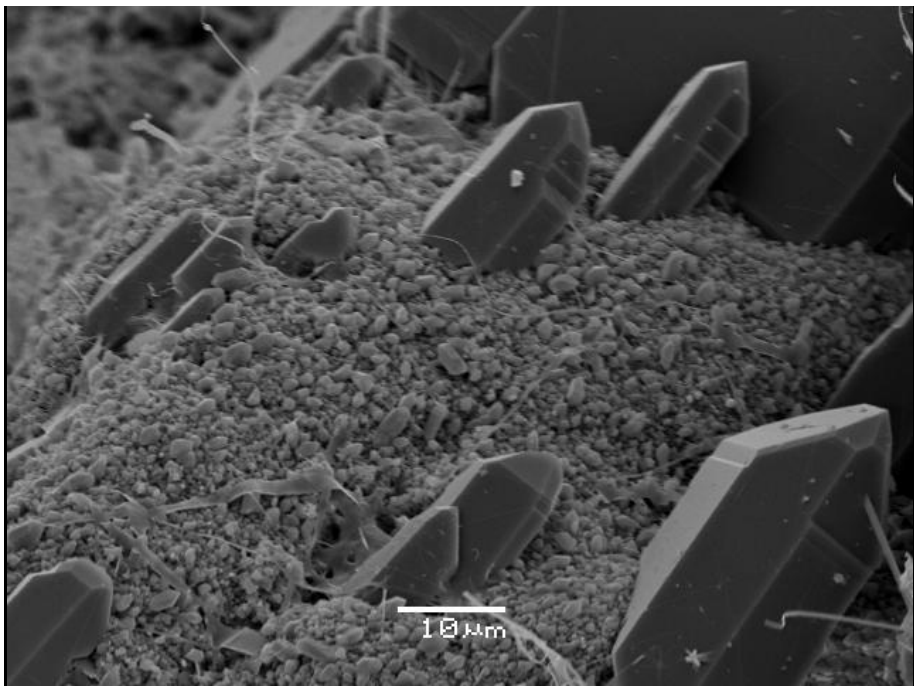

UNIVERSITY OF OSLO

FACULTY OF MATHEMATICS AND NATURAL SCIENCES

Reservoir Quality in the Jurassic sandstones reservoirs located in the Central Graben

A sedimentological and petrophysical approach

Ali Mustafa Khan Niazi

Master Thesis in Geosciences

Discipline: PEGG

Department of Geosciences

Faculty of Mathematics and Natural Sciences

UNIVERSITY OF OSLO

17.06.2011

Tutor(s): Jens Jahren
This work is published digitally through DUO – Digitale Utgivelser ved UiO
http://www.duo.uio.no
It is also catalogued in BIBSYS (http://www.bibsys.no/english)

ACKNOWLEDGMENTS

I feel instigated from within to extend my steadfast thanks to ALMIGHTY ALLAH whose magnanimous and chivalrous blessings enabled me to perceive and purse my ambitions and objectives. Special praises to Prophet Muhammad PBUH, who is bellwether for humanity as a whole.

I feel great honor in expressing my avid gratifications to my supervisor Jens Jahren, under whose dynamic supervision, auspicious and considerate guidance, encouragement and altruistic attitude, I was able to accomplish work presented in this dissertation.

I also extend my special thanks to Phd Student Tom Erik Mast for his esteemed guidance, suggestions, discussion and professional support throughout my thesis work. I also thank to Berit Løken Berg for always being supportive and helpful in my SEM studies. Without her help I believe my project was incomplete.

Special thanks to my all friends at University of Oslo who will be missed with lunch and coffee breaks.

In the end my whole hearted and incessant gratitude to my loving parents, my brother and my sister, who always appreciated, encouraged, and helped me during my eighteen years of studies.

June, 2011

Ali Mustafa Khan Niazi

ABSTRACT

This study investigates the diagenesis and reservoir quality of Upper Jurassic Sandstones from the Central Graben. Petrophysical and petrographical studies have been done on cored interval from well 2/1-6.

Precipitation of quartz cement is the main porosity destroying process in deeply buried quartz rich sandstone reservoirs of the North Sea. Quartz cement precipitate in the form of syntaxial overgrowth over detrital grain of quartz. Grain coatings like micro-quartz and illite are the main reasons of preservation of porosity in the area. Grain coats preserve porosity by covering the grain and inhibiting the quartz overgrowth.

Petrographical and petrophysical data in this study clearly indicates that grain coatings are present in the Central Graben. Micro-quartz grain coating is the most common grain coat in the Upper Jurassic Sandstones of Ula Formation. Micro-quartz grain coat are generated from the transformation of siliceous sponge spicules known as Rhaxella Perforata. Though micro-quartz is present in all low and high porosity zones but it could not preserve porosity in low porosity zones. Clay grain coats like illite and chlorite grain coats are also present but in variable amounts.

Relation between Intergranular volume (IGV) vs matrix and quartz cementation vs porosity have been also been studied. IGV is strongly affected by mechanical compaction, grain size, grain shape, quartz cementation, and carbonate cement. Sandstones with high amount of matrix and fine grained grains have high IGV as compared to coarse grained sandstones because coarse grained sandstones are compacted more when they are subjected to mechanical compaction.

Grain shape has also a pronounced affect on the porosity in the area. Angular grains loose porosity as they are subjected to stress. In angular grains contact forces are more concentrated because of small contact areas. This is the reason we have low porosity zones which have angular grains and were not influenced by micro-quartz grain coatings.

TABLE OF CONTENTS

CHAPTER 1: INTRODUCTION

1.1. INTRODUCTION

This thesis is a collaboration between Det Norske oljeselskap ASA and the Department of Geosciences at University of Oslo. The aim of this thesis is to increase the understanding of the distribution and quality of deeply buried Jurassic Sandstone Reservoirs located in the Central Graben.

Cementation is the main cause of the drop in reservoir properties of Jurassic sandstones from the North Sea which are buried deeper than about 3000m (70 to 100° C). Cementation is a process that is strongly controlled by temperature and kinetics. In deeply buried reservoirs (>4000m/140°C) a good understanding of the factors controlling the cementation exists since normal quartz cementation would normally lead to limited reservoir properties at similar depths. Reservoir quality in the deeply buried sandstone prospects therefore depend on factors preventing or delaying the quartz cementation. These factors include the grain coatings like chlorite and micro-quartz (Bjørlykke, 2010).

1.2. PURPOSE AND METHODS

The main objective of this thesis is to characterize the cored reservoir interval of well 2/1-6 of Gyda Field. Main objective also includes providing valuable and essential information on reservoir quality as a function of quartz cementation and porosity preserving mechanisms in Upper Jurassic Sandstones in the Central graben which are buried to depths > 4Km. This will be done by integration of methods on two levels of investigation:

i. Well correlation and petrophysical evaluation

ii. Petrographic analysis of thin sections (Optical Microscopy and SEM)

1.3. STUDY AREA

The study area is located in the Central Graben within the North Sea in block 7/12, 2/1, and 1/3 belonging to Ula, Gyda and Tambar fields respectively (Figure 1). These blocks are located in Cod Terrace which are affected by Triassic salt tectonics (Gowers et al, 1993). These blocks are located in southern part of the North Sea (Figure 1.1).

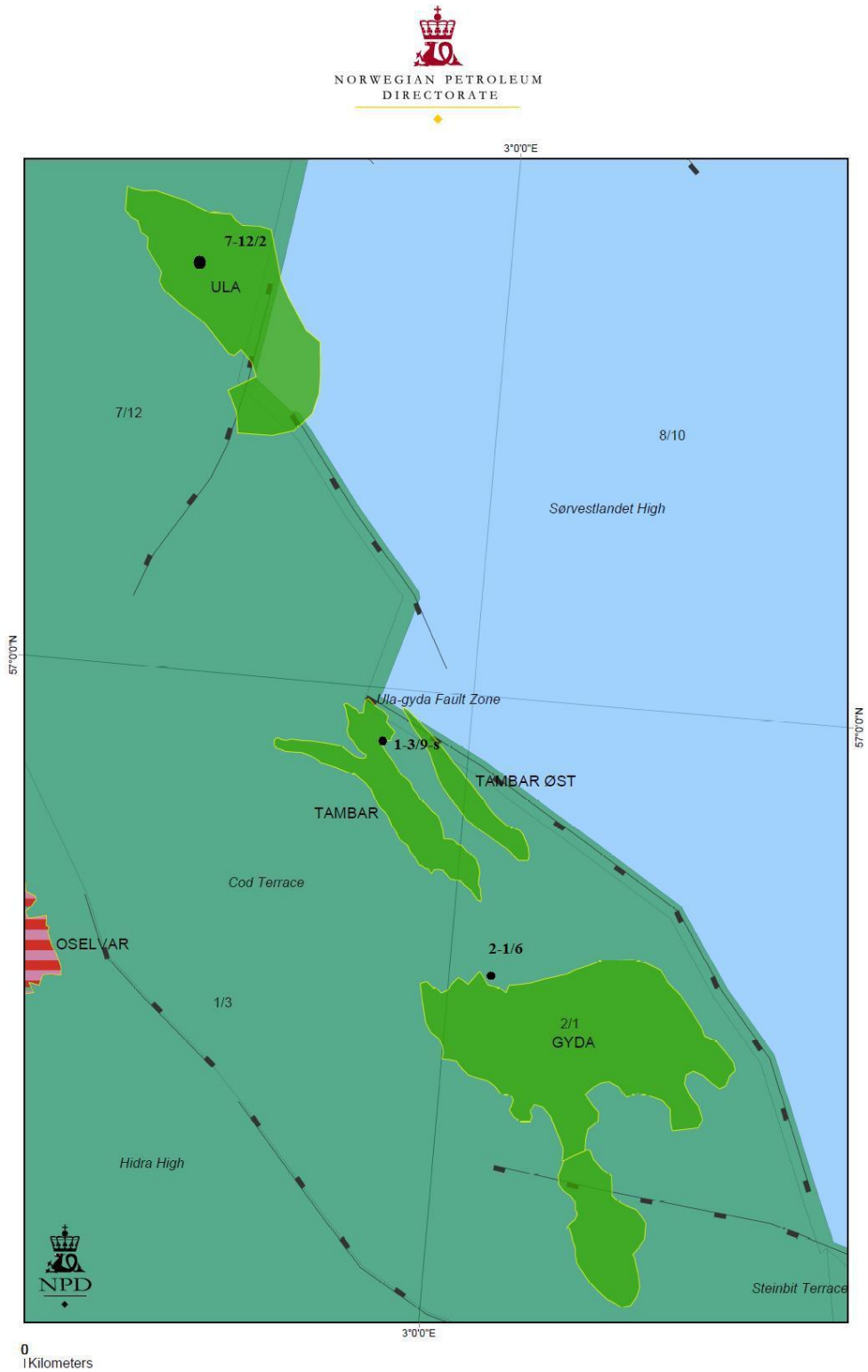

Figure 1.1: Structural element map of the study area. Black dots indicate the well location (Map modified from NPD 2011).

CHAPTER 2: GEOLOGIC FRAMEWORK OF THE CENTRAL GRABEN

2.1. INTRODUCTION

The Central Graben is located in the middle and southern part of the North Sea (Figure 2.1). The term The Norwegian Central Trough was first introduced by Ronnevik et al. (1975). In Norway, the Central Trough is the official nomenclature although "Central Graben" is more accepted (Gowers et al. 1993).

Structural configuration of North Sea is predominantly controlled by Late Jurassic to Early Cretaceous rifting events (Figure 2.1). The North Sea rift systems has a prolonged extensional history that began in Permo-Triassic and further continued during Jurassic and Early Cretaceous, followed subsequently by respective thermal cooling and subsidence stages (Zanella & Coward, 2003; Ravnas et al., 2000).

A large amount of literature has been published on the geology and tectonic evolution of the North Sea (e.g. Brooks and Glennie, 1987; Deegan and Scull, 1977; Gabrielsen, 1986; Glennie, 1998; Nøttvedt et al., 1995; Vollset and Dorê, 1984). This chapter will focus mainly on the Central Graben area. For further reading the Millennium Atlas (Evans et al., 2003) and references given gives a complete description of the petroleum geology of the North Sea.

2.2. STRUCTURAL SETTINGS

The Central Graben is the southern arm of the triple junction between Viking Graben, the Central Graben and the Moray Firth basins (Figure 2.1). The Central Graben is more symmetrical in character as compared to the Viking Graben and the Moray Firth basin which are asymmetrical in character (Zanella and Coward, 2003).

The Central Graben is characterized by several narrow discontinuous structural highs and lows (Skjerven et al., 1983). As mentioned above Central Graben is symmetrical in character but it has a very complicated tectonic history. Its tectonic history involves oblique/strike slip movements and structural inversion (Sears et al. 1993). Different researchers have proposed different models to explain the tectonic framework of the Central Graben (Beach (1986), Gibbs (1989), Roberts and Yielding (1991) and Roberts et al. (1990)). This thesis will follow the structural framework proposed by Gowers et al. (1993).

According to Gowers et al. (1993) development of Central Graben can be divided in to three different stages. Stages of evolution of Central Graben are shown in Figure 2.2. These stages are:

1) Late Triassic to middle Jurassic flexural uplift

2) Late Jurassic to early Cretaceous fragmentation

3) Late Cretaceous to Tertiary flexural subsidence

First stage is highly influenced by Halokinetics. Salt Tectonics has been recognized in Central Graben in early phases of exploration in the area due to the fact that various diapirs penetrate into late Tertiary sediments. Major movements of salt occurred in end of Triassic time by Zechstein salt deposits. These halokinetic movements resulted in series of highs and ridges with the intervening blocks of Triassic sediments resting on thin salt or on Permian pre-salt deposits. Flexural uplift caused by movement of salt is evident by thinning of Triassic and early Jurassic sediments towards the Central Graben and thinning of middle Jurassic sediments (Gowers et al. 1993). Salt movement in Central Graben had a great influence on the distribution of Reservoirs (Smith et al. 1993).

Second stage involves the fragmentation of Central Graben which started in Oxfordian with intense faulting and continued to middle Cretaceous. In this stage, tectonic movements were totally confined to Central Graben with very little influence of movements outside the graben. In Volgian, a major change in tectonic deformation occurred. In this time, faulting became dominant and this faulting rotated the individual fault blocks. This caused erosion on footwalls and deposition in hanging walls. This is evident by the dips away from the axis of graben. These rotational movements are more intense and best seen in Hidra High (Gowers et al. 1993).

The rotational movement in Central Graben rapidly ceased in late Volgian with initiation of regional subsidence causing the high areas to drown below the wave base. Distribution of these lower Cretaceous sediments is still not well understood, but there are many evidences which lead to renewed basin subsidence in early Cretaceous. It is unclear that this subsidence is of syn-depositional age is of the lower Cretaceous. Sediments were deposited in the basins created in

late Jurassic. Basins formed due to early Cretaceous subsidence are fault bounded, flexure bounded, and have undisturbed internal geometry (Gowers et al. 1993).

Flexural subsidence is third stage of tectonic events which resulted in formation of Central Graben and these events are related to Thermal Subsidence (McKenzie, 1978). This type of subsidence in Central Graben is caused by thermal cooling of crust in late Cretaceous time. Thermal subsidence is best seen in Breiflabb Basin but can not be seen in Søgne Basin or Tail End graben (Gowers et al. 1993).

2.3. STRUCTURAL ELEMENTS

The Central Graben is trending in NW-SE direction and consists of two troughs towards east and west of intrabasinal Forties-Montrose and Josphine highs. These highs make up the spine between two sub-basins as shown in Figure 2.1 (Zanella and Coward, 2003). Central Graben can be considered as a series of north-south sub-basins, which offsets along Tornquist basement lineaments to west-north-west direction (Erratt et al., 1999). Complex pattern of the Central Graben becomes complicated by presence of the thick Zechstein evaporites (Zanella and Coward, 2003).

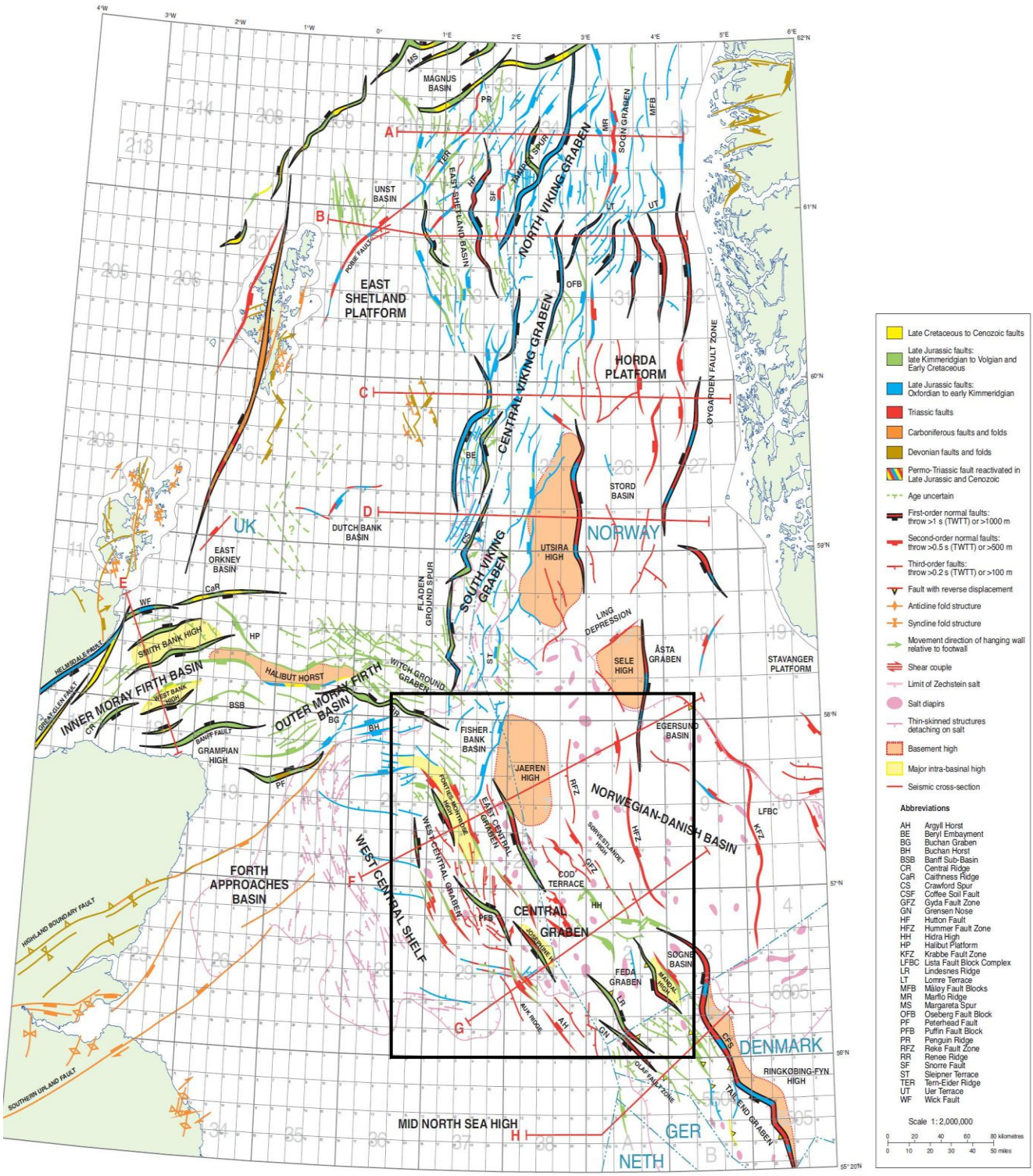

Figure 2.1: Regional structural map of North Sea modified after Zanella and Coward, 2003.

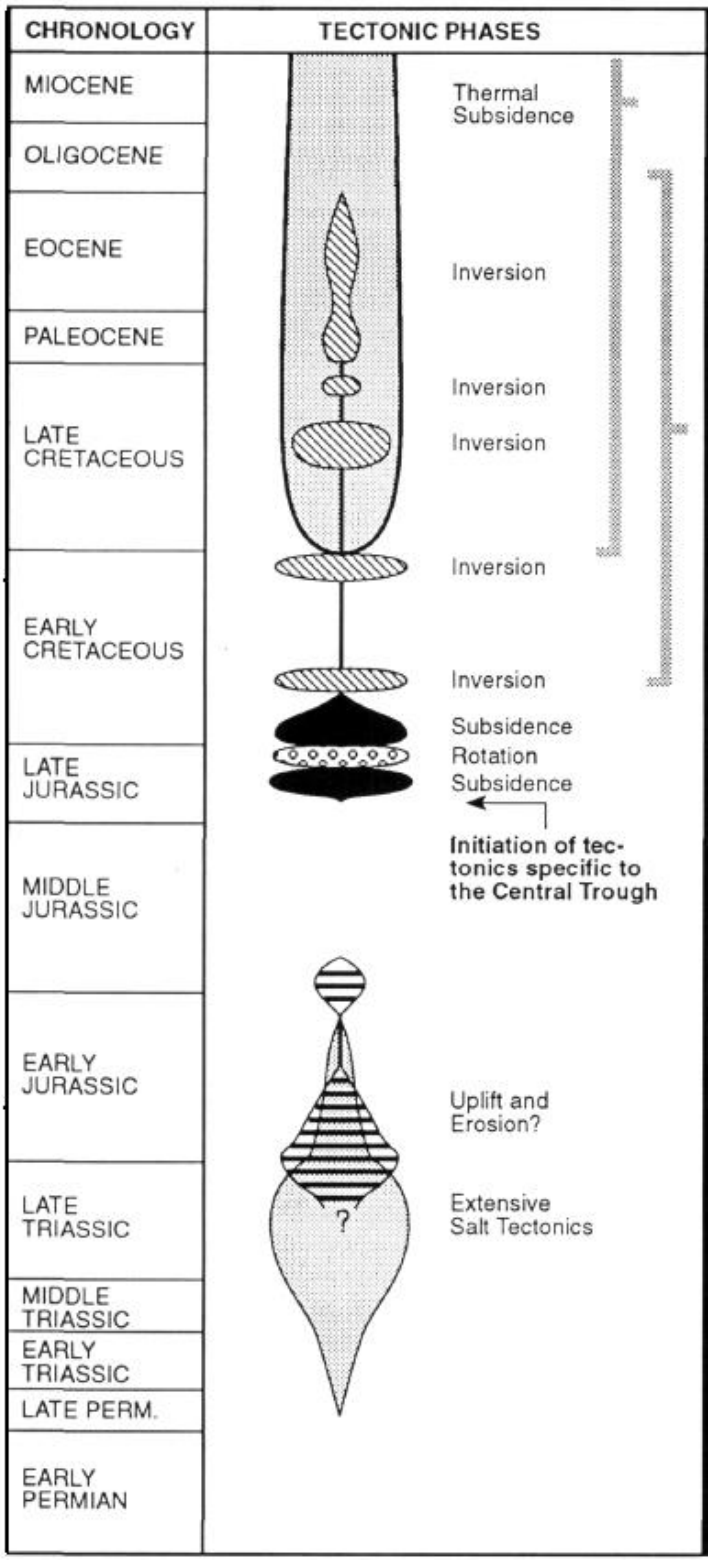

Figure 2.2: Schematic illustration describing the evolution of the Central Graben (modified after Gowers et al. 1993).

2.4. STRATIGRAPHIC SETTING

Late Jurassic is rightly considered as the most important period in evolution of the North Sea petroleum system because Kimmeridge Clay Formation and its equivalent were deposited which are the major oil source rocks in the North Sea (Cornford, 2009). The complex tectonic history of Central Graben created vast majority of hydrocarbon traps, which were to be filled with hydrocarbons upon maturation of Kimmeridge Clay and its equivalents later. Therefore, Late Jurassic becomes the single most significant period in the overall development of petroliferous North Sea basin (Fraser et al., 2002).

Upper Jurassic hydrocarbon play's nature was controlled mainly by progressive evolution and decay of Late Jurassic to Early Cretaceous rifting. Depositional and structural processes related to rifting had a main bearing on distribution of source rocks, seal and reservoirs in the basin and on the development of hydrocarbon trapping configurations (Fraser et al., 2002). According to Fraser et al (2002), the petroleum play of Central Graben is characterized by two types of reservoirs: Coastal Shelf Sandstones and Deep Sea Submarine-Fan Sandstones in the form of basin floor fans. Erratt et al (1999) postulated that these good quality reservoirs are distributed in Central Graben, Viking Graben and Moray Firth Graben systems which display a good interplay between depositional and structural processes.

This chapter will focus on the sandstones deposited in Shallow marine/Coastal Shelf Depositional System. As Ula Formation on which this study is based was deposited in this system (Fraser et al., 2002). Stratigraphic overview of the Norwegian Central Graben is shown in Figure 2.3.

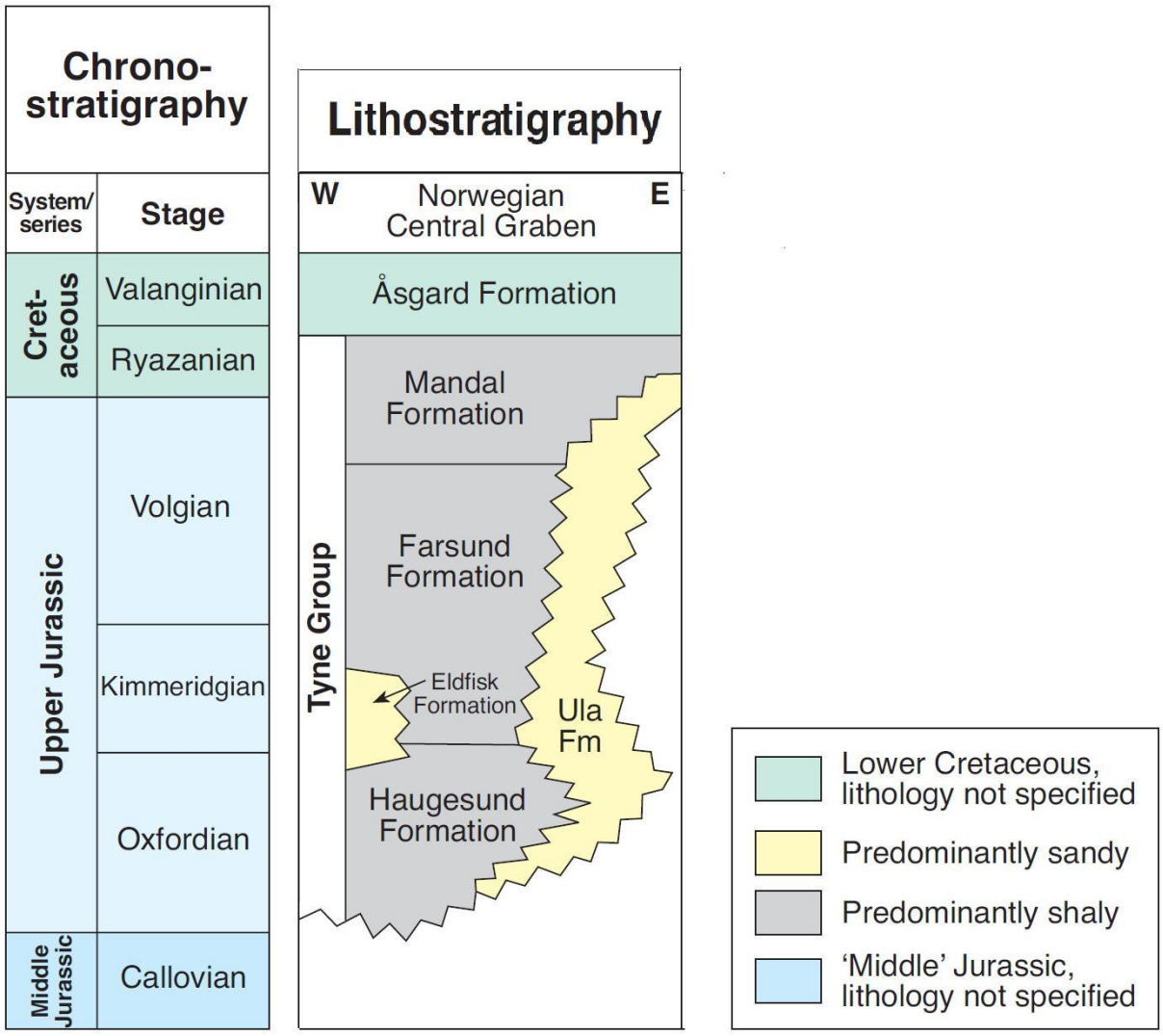

Figure 2.3: Showing stratigraphic overview of the Norwegian Central Graben (Modified after Fraser et al. 2002)

2.5. Upper Jurassic Depositional System As Shallow Marine/Coastal Shelf Depositional Systems

Following rifting, sea level rose rapidly during Jurassic time which caused development of an extensive coastal shelf depositional system. This type of depositional system resulted in high reservoir quality shallow marine sands at the basin margins. These sands include Emerald, Fulmar, Heno, Hugin, Piper, Sognefjord and Ula Formations. In Oxfordian and Kimmeridigian times (Late Jurassic), the depositional pattern was progressive retrogradation of coastal shelf

depositional system (Figure 2.4) (Fraser et al., 2002). These shallow marine sandstones are though different in ages but their physical characteristics are similar. They have been extensively bioturbated so internally they are structureless. They have wide range of ichnofacies which helps a lot in reconstructing their depositional environments and palaeobathymetry (Pemberton et al., 1992; Taylor and Gawthorpe, 1993; Martin and Pollard, 1996).

Primarily, reservoir quality is controlled by its parent depositional processes until reservoir is buried deep. Such processes control sorting, packing of grains, cementation and primary sedimentary features that eventually determine the type of porosity and to a certain extent the permeability within the reservoir (Cannon and Gownland, 1996). In Central Graben, good quality sandstones are lying in upper parts of upward-coarsening progradational cycles which were deposited in high energy environment, influenced by storm waves. In deeper parts porosity is preserved by high overpressures along with some secondary porosity (Fraser et al., 2002).

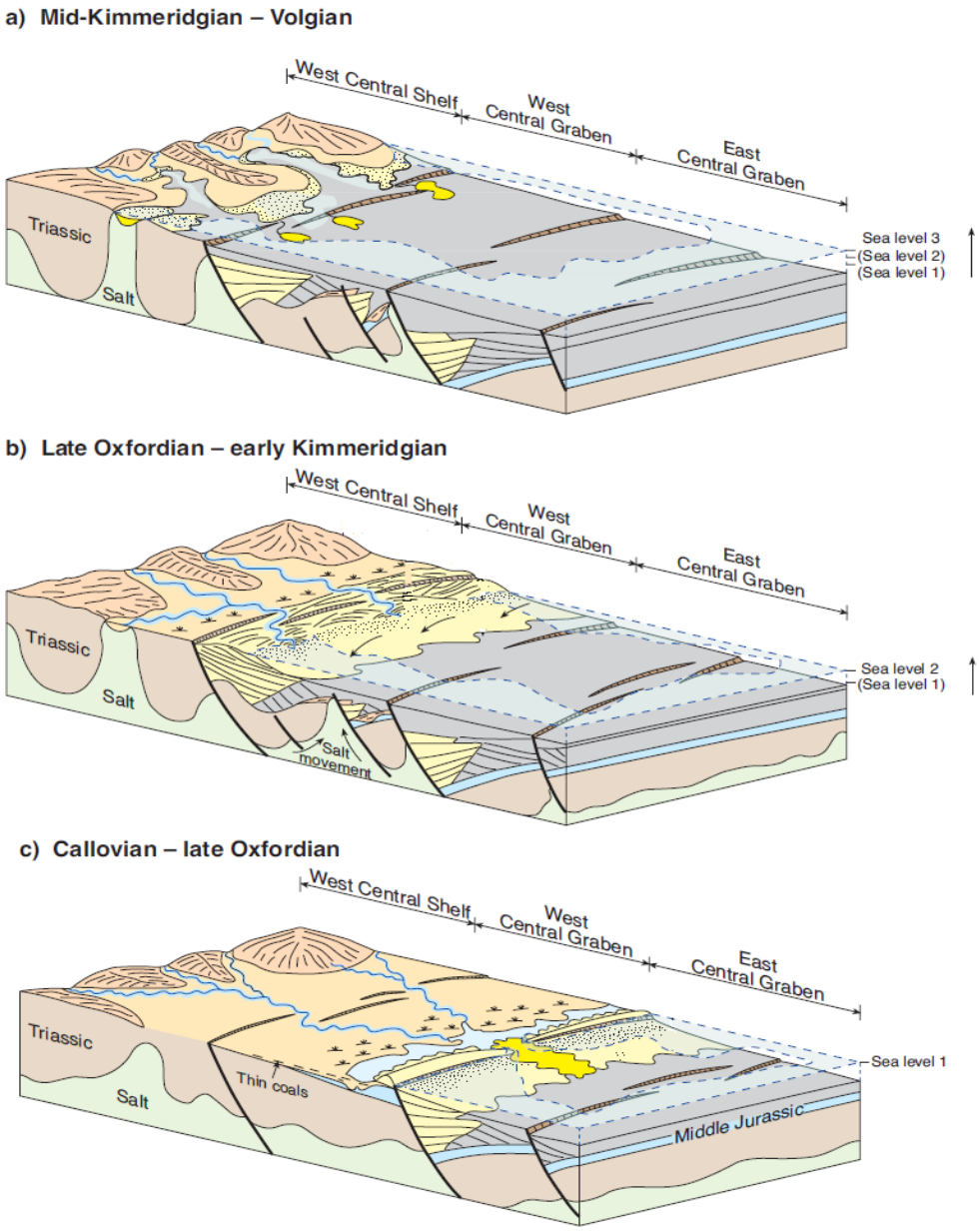

Figure 2.4: Schematic models for the development of Fulmar Formation Sandstones in the Central Graben. Modified after Fraser et.al, 2002.

CHAPTER 3: THEORETICAL BACKGROUND

3.1. INTRODUCTION

Properties of sandstone depend on its composition at shallow depth, and on temperature and on stress history during burial. Start of diagenetic process depends on the initial composition of sandstone. Initial composition in turn depends on the provenance, transport and depositional environments. The most important factor in predicting reservoir quality at depth is the initial or primary clastic composition and the depositional environment (Figure 3.1) (Bjørlykke, 2010, p115).

According to Bjørlykke, 2010, main diagenetic processes are:

(1) Near surface diagenesis.

(2) Mechanical compaction

(3) Chemical compaction

(4) Cementation

3.2. NEAR SURFACE DIAGENESIS

When sediments are deposited, composition of sediments starts to be modified by diagenetic reactions. At burial depth of about <1 to 10 m, sediments are most susceptible to react with water or air or both by process of fluid flow and diffusion. Near surface, diagenesis is caused by meteoric water inflow which is actually fresh and is unsaturated with respect to minerals. When fresh water seeps down in soil, it starts to react and dissolve carbonates and other unstable minerals in nature like feldspar and mica. (Figure 3.2) (Bjørlykke, 2010, p118). Two chemical processes at this stage are of significant importance which are carbonate cementation and K-feldspar leaching.

At shallow depth carbonate cement is mainly derived from biogenic carbonates within the rock. This biogenic carbonate becomes unstable below the redox boundary. Due to high reaction rates of carbonate minerals, carbonates dissolve and re-precipitate as cement at shallow burial depth (Saigal and Bjørlykke, 1987). Carbonate minerals available in rocks depend on biological

productivity. Biological productivity in turn depends on clastic sedimentation rate. Carbonates are very common in sandstones of Upper Jurassic and younger in age.

Reservoir properties are known to be significantly affected by leaching of K-feldspar, mica and precipitation of kaolinite (Bjørlykke et al., 1992). In the presence of K-feldspar, kaolinite is thermodynamically unstable. Later, during deep burial (120-140˚C) kaolinite will be transformed into illite. The transformation of kaolinite into illite affects the permeability of rock while leaching of K-feldspar causes an increase in secondary porosity (Bjørlykke, 2010).

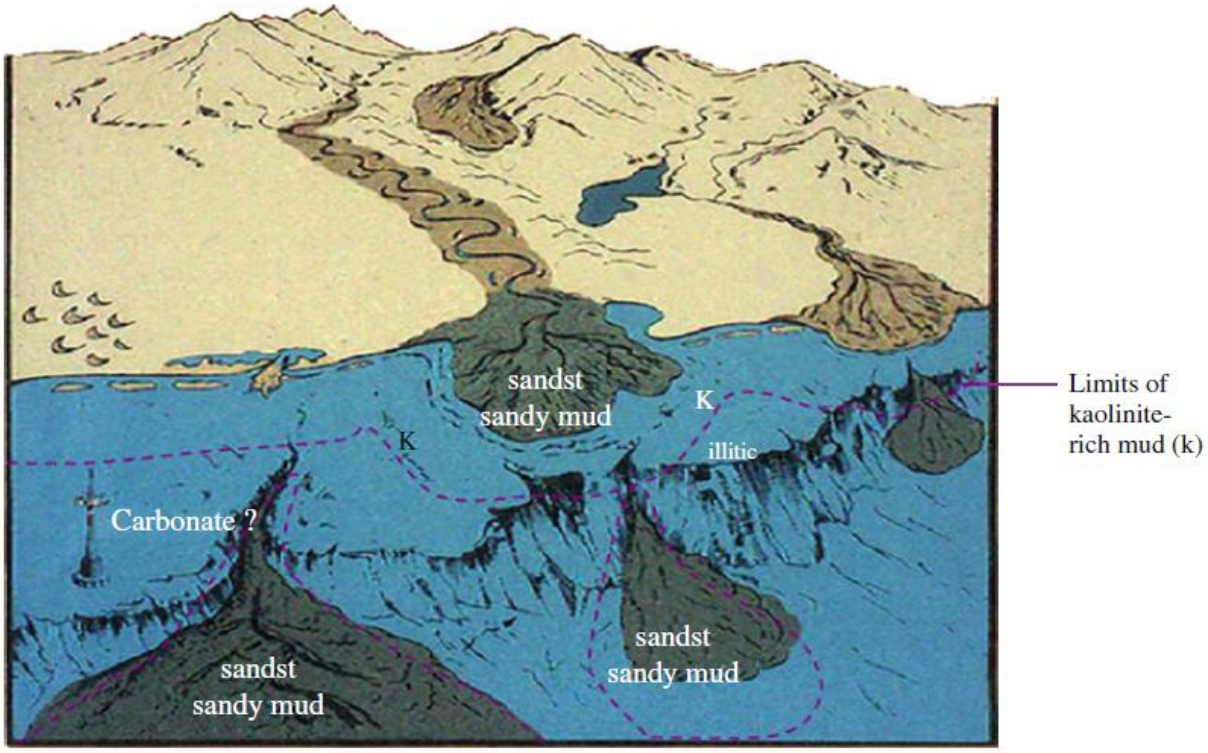

Figure 3.1: Schematic illustration of a sedimentary basin on a continental margin (Bjørlykke, 2010, p115).

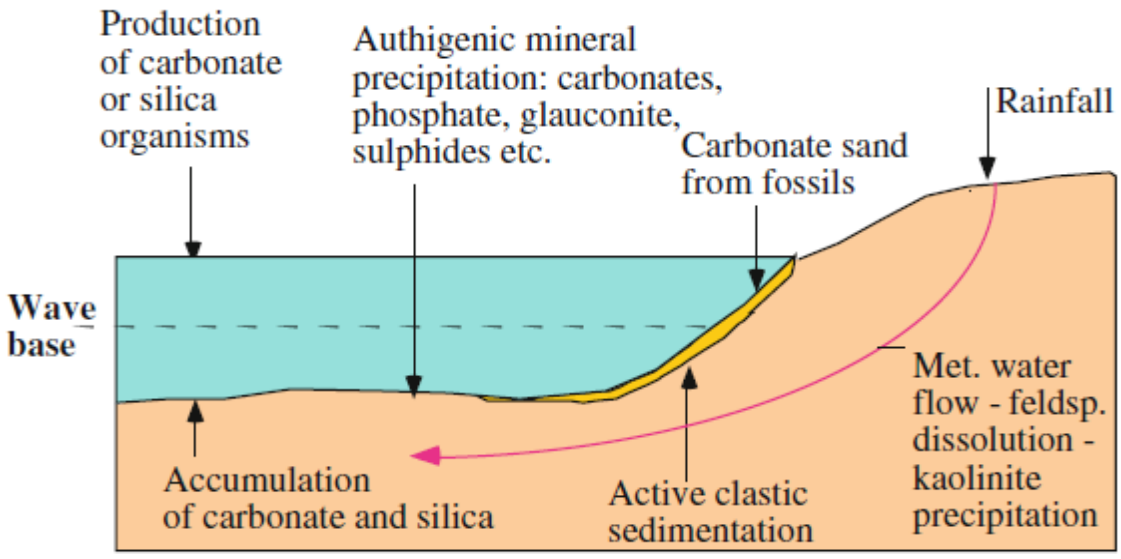

Figure 3.2: Showing diagenetic processes in shallow marine environment (Bjørlykke, 2010, p118).

These reactions of water with feldspar and micas can be written as follows (Bjørlykke, 2010):

$$2K(Na)AlSi_3O_8 + 2H^+ + 9H_2O \longrightarrow Al_2Si_2O_5(OH)_4 + 4H_4SiO_4 + 2K + (2Na^+)$$

Feldspar — Kaolinite — dissolved silica — dissolved cations

$$2KAl_3Si_3O_{10}(OH)_2 + 2H^+ + 3H_2O \longrightarrow 3Al_2Si_2O_5(OH)_4 + 2K^+$$

Muscovite — Kaolinite

3.3. Mechanical Compaction

Grain size, sorting, shape and matrix content determine the initial space among the sand grains, measured as the intergranular volume (IGV) of the sediment (Paxton et.al, 2002). As sediments are buried, IGV decreases, which is function of mechanical compaction. Mechanical compaction causes grains to pack closely together (Ajdukiewicz and Lander, 2010). Experimental compaction shows that initial porosity (40-42%) of sandstone may reduce to 35-25% at 20-30 MPa (2-3 Km depth). This depends on grain strength and grain size (Chuhan et al, 2003).

3.4. Sandstone Reservoirs Buried to Intermediate Depth (2.0–3.5 km, 50–120◦C)

Quartz cementation starts at intermediate depth (2.0-2.5 Km), which thus increases the strength of the rock and stops mechanical compaction. From this depth onwards, chemical compaction will be the main process acting on the reservoir. 2-4% quartz cement will stop mechanical

compaction and strengthen the rock. This means chemical compaction will be the main process acting on the reservoir. Albitization is also an important process that may alter composition of reservoirs buried at this depth (Bjørlykke, 2010, p122).

Generally in basins the geothermal gradient is 30-35° C/Km. In sandstones where temperature reaches 60 to 80 °C, quartz cementation starts to precipitate and starts to modify porosity. Quartz cementation depends on time, temperature (as shown in Figure 3.3) and surface area available (Ajdukiewicz and Lander, 2010 and Walderhaug, 1996). In both mechanical compaction and chemical compaction porosity is decreased. Quartz cementation is limited by diagenetic clay coats over grains. Quartz cementation is main porosity destroying process in sandstones buried at intermediate depth (2.0-3.5 Km) (Bjørlykke et al., 1989). Quartz cementation will be discussed in detail later within this chapter.

At intermediate burial depth, K-feldspar may be albitized and this is an important diagenetic process which may result in significant change in composition of sandstone reservoirs. K-feldspar reacts with Na^+ which results in Albite and release of K^+ (Bjørlykke, 2010). This reaction is shown below:

$KAlSi_3O_8 + Na^+ \longrightarrow NaAlSi_3O_8 + K^+$
K-feldspar Albite After Saigal et al. (1988)

According to Saigal et al (1988) albitization starts at about 65˚ C to 105˚ C which clearly corresponds to 2-3 Km burial depth. 30-50% of original K-feldspar can be albitized (Aagaard et al., 1990).

3.5. Deeply Buried Sandstones (>3.5–4 km, >120◦C)

As quartz cementation starts, it doesn't stop till all porosity is filled by quartz cement until temperature falls below 70 to 80°C due to uplift or other reasons (Walderhaug, 1996). During continuous burial, quartz cementation continues till available porosity is lost and when temperature reaches 200-300°C sandstone converts into hard quartzite. This process may take millions of years (Bjørlykke, 2010, p126).

Illitization is a process which takes place at burial depths of about 3.7 to 4 Km (120-140°C). This process only starts if Kaolinite and K-feldspar are present together in reservoir (Chuhan et al., 2000). As mentioned earlier Kaolinite and K-feldspar are thermodynamically unstable when they are present together in the reservoir. But for illitization, high activation energies are required which are available at deep burial. Along, with quartz cementation, illitization is probably the most important reasons for reduction of reservoir properties (Bjørlykke et al., 1992). The illitization of Kaolinite can be written as following equation:

$$2K(Na)AlSi_3O_8 + Al_2Si_2O_5(OH)_4 \longrightarrow KAl_3Si_3O_{10}(OH)_2 + SiO_2 + 2H_2O$$

K-feldspar Kaolinite Illite Quartz

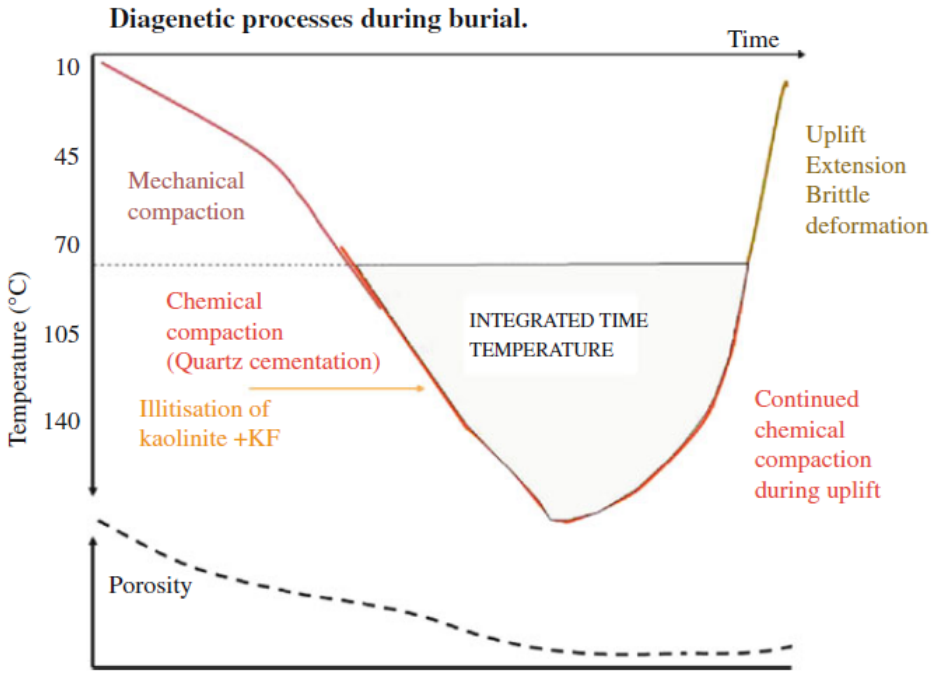

Figure 3.3: Diagenetic processes, mainly quartz cementation, as a function of temperature and time. Note that quartz cementation will continue also during uplift as long as the temperature exceeds 70–80◦C (Bjørlykke, 2010, p126).

3.6. QUARTZ CEMENTATION

According to Worden and Morad (2000) reservoir quality depends on three factors:

1) Porosity and Permeability

2) Degree of mechanical and chemical compaction

3) Amount and type of pore filling cement.

Sandstone reservoirs buried to 2-3 Km depths looses their porosity from 35-45% (depositional porosity) to 15-20%. The main reason of porosity reduction at this depth is quartz cementation which kicks off at 70-80°C (Bjørlykke et al., 1989).

3.6.1. ORIGIN OF QUARTZ CEMENT IN SANDSTONES

The main sources of silica have been unclear till late 90's with variety of different suggestions and explanations (e.g McBride, 1989). These ideas mainly included external sources and dissolution process. External source is mainly considered a large flux of water in sandstone. But later it was proved that external sources have no role in quartz cementation. Bjørlykke (1994) calculated that 10^8 cm^3 water passing through each cm^2 of sandstone body will result in quartz cementation. This is naturally impossible to occur. Most of the authors believe source of silica is mainly by the illite-mica induced dissolution which was introduced by Oelkers et al. (2000). It is also abbreviated as I-MID.

"Dissolution at grain contacts requires stress, and the process is often called Pressure Solution, but the degree of stress needed is relatively moderate" (Bjørlykke, 2010, p125). Rutter and Elliott (1976) introduced that pressure has the key control on the silica solubility. However, Bjørkum (1996) emphasized on the critical role of the temperature and negligible role of pressure for silica dissolution in diagenetic rocks. Contacts between illite clay or mica and quartz grain are the preferred sites of dissolution (Fisher et al., 2000). These contacts are called stylolites. Silica dissolved at the stylolites is transported by the process of diffusion to grain surfaces where it forms quartz overgrowth. Precipitation will take place away from the stylolites where the silica will be oversaturated with respect to quartz (Bjørlykke, 2010, p125).

Sandstones of ages from Upper Jurassic have considerable amounts of siliceous and opaline fossils. Rhaxella perforata is most common siliceous fossil. These fossils are dissolved to produce high supersaturation of silica (Bjørlykke, 2010). Quartz cement which results from the dissolution of the biogenic sources results in microcrystalline grain coats and mesocrystalline quartz overgrowth (Vagle et al., 1994; Hendry and Trewin, 1995).

3.6.2. FACTORS INFLUENCING QUARTZ CEMENTATION

Temperature effects quartz cementation in two ways. First it can affect the diagenetic processes which result in release of silica. Secondly it can affect quartz dissolution, diffusion and precipitation. Thus "Temperature affects both the thermo-dynamics and the kinetics of geochemical process that cause quartz cementation". Rate of quartz cementation is increased exponentially by a factor of 1.7 for every 10°C as a function of temperature (Walderhaug 1996). To start quartz cementation, reservoir must attain temperature of about 60°C. Before this temperature (1.5-2Km depth) quartz cementation doesn't start (Bjørlykke, 2010). Precipitation of quartz cementation and quartz overgrowth increases during deep burial diagenesis (>2.5 km) with temperatures 90-130°C (Giles et al., 1992; Gulyas et al., 1993). Precipitation of quartz cement is also a function of surface area available as quartz cementation reduces porosity. So to precipitate more quartz cement, porosity will be required. Basins which are subsiding slowly, may witness quartz cementation for tens of millions of years at low temperatures (<100°C). Inversely at high temperatures cementation may take place for shorter time span (Morad et al., 1994).

3.7. PRESERVATION OF POROSITY

In sandstones, early formation of grain coats on quartz grains inhibits the quartz cementation and prevents porosity loss. Grain coats mostly observed in sandstone are clay coats and microcrystalline quartz (Taylor et al., 2010).

3.7.1. CLAY COATS

Clay minerals are considered important and are recognized in sandstones for preserving porosity in many studies (Heald and Larese, 1974; Thomson, 1979; Pittman et al., 1992; Ehrenberg, 1993; Bloch et al., 2002; Anjos et al., 2009; Taylor et al., 2004). These all studies have shown that sandstones where poor clay coats are developed have very low porosity because of quartz cementation and sandstones with a lot of clay coats contains less amount of quartz cementation and high porosity. Clay coatings include Illite, Smectite, and Chlorite. Authigenic chlorite is most important grain coating which is effective in controlling quartz cementation. This is due to the tendency of chlorite to form continuous layers between the quartz grain and the pore space

(Taylor et al., 2010). Bloch et al. (2002) proposed that other types of clay coatings around quartz grains don't stop quartz cementation as much as a coating of chlorite does. Numerical models of quartz cementation given by Bloch et al. (2002) and Lander et al (2008) proves that reservoirs which are deeply buried and are at higher temperatures require full grain coats to preserve porosity.

3.7.2. MICROCRYSTALLINE QUARTZ COATS

Microcrystalline quartz coats over quartz grains prove to be an effective way to preserve porosity in sandstones (Aase et al., 1996). As microcrystalline quartz is very small in size so it cannot be easily detected in thin section using standard optical microscopes but can be very easily detected in Scanning Electron Microscope (SEM). Micro-quartz is usually the result of rapid crystallization of silica from a silica-supersaturated solution. Dissolution of siliceous sponge spicules help in maintaining the dissolved silica supersaturation even at very low temperatures (Taylor et al., 2010). Numerous examples of microcrystalline quartz over grains of deeply buried sands are available from Jurassic and Cretaceous intervals of the North Sea (Aase et al., 1996; Ramm et al., 1997; Jahren and Ramm., 2000; Aase and Walderhaug, 2005). These studies show that small amount of microcrystalline quartz has preserved porosity and inhibited quartz overgrowth and quartz cementation.

Presence of micro-quartz grain coatings is always pointing to the presence of amorphous silica precursor Rhaxella Perforata (Maliva and Siever, 1988). In 1890, Hinde reported spicules and specimens of Rhaxella Perforata belonging to the Lower Cretaceous Grit Formation (Lower Oxfordian) from Yorkshire, England. Sponge spicules and Rhaxella Perforata are commonly reported in onshore England and sandstones of Upper Jurassic to Lower Cretaceous of the North Sea (Table 3.1). In the North Sea, Rhaxella spicules are abundant in shallow marine deposits e.g Alness Spiculite Member and the Fulmar Formation. They are also reported from deep marine turbiditic reservoirs e.g Scapa, Ten foot turbidites. Ula Formation is also reported to have Rhaxella Perforata which was deposited in Shoreface, offshore bar environment (Ramm and Forsberg, 1991, Vollset and Dorê, 1984).

Sedimentary reworking of sponge spicules is very important as a distributing mechanism of Rhaxella Spicules in shallow marine sandstones. Wilson (1968) reported spicules from shallow marine environment sandstones of Oxfordian age from onshore southern England.

3.7.3. HYDROCARBON INCLUSION

Many years ago, Johnson (1920), proposed an idea that hydrocarbons as pore fluid in sandstone can influence porosity. Until recently it has been thought that in reservoir with hydrocarbons, porosity was preserved (Emery et al., 1993; Gulyas et al., 1993). However recently it has been known that effect of hydrocarbon emplacement in sandstones has been over stated (Aase and Walderhaug, 2005; Barclay and Worden 2000b; Giles et al., 1992; Ramm and Bjørlykke, 1994; Walderhaug, 1994a).

Fractional amount of water in sandstone is called Water Saturation (Sw). The Sw of a rock is equal to the height above the oil-water transition zone and the rock fabric. Wettability of the reservoir also affects the values of Sw. Wettability is defined as the ability of rock to allow oil to come into contact with the grain surface. Sandstones contain a variety of minerals so it has mixed Wettability. Quartz, feldspar and illite are susceptible to water-wet behavior (Fassi-Fihri et al., 1991). While kaolinite and chlorite are susceptible to being oil wet (Sincock and Black, 1988; Fassi-Fihri et al., 1991; Barclay and Worden, 2000b). Sandstone reservoirs which are water-wet, the presence of oil in the sandstones will have no affect on the precipitation of quartz cement because the surface of quartz grain will be coated by water. In comparison, oil-wet systems, the surface of quartz grain will be coated with oil, the pore water will have no ability to precipitate quartz cement and overgrow the quartz grain (Worden and Morad, 2000).

Location	Formation / Member	Age	Depositional environment	Reference
southern England	Corallian beds	Oxfordian	Sediment starved lagoon	(Talbot, 1973; Wilson, 1968)
Moray Firth	Alness Spiculite Member	Mid Oxfordian	Large subtidal shoal	(Andrews and Brown, 1987)
Scapa Field (Moray Firth)	Scapa Member	Valanginian – late Hauterivian	Turbidites	(Hendry and Trewin, 1995)
Brora (Inner Moray Firth)	Brora Arenaceous, Brora Argillaceous	Oxfordian – callovian	Coastal sand bar: Tidal sand waves	(Vagle et al.,1994)
Moray Firth (Claymore Field)	Cimmeridge Clay Formation Formation (Ten Foot turbidites)	Kimmeridgian – early Tithonian	Turbidites	(Spark and Trewin, 1986)
Central Viking Graben (Fulmar Field)	Fulmar Formation	Kimmeridgian – Oxfordian	Highly bioturbated, shelf - lower shoreface	(Gowland, 1996; van der Helm et al., 1990)
Central Viking Graben (Ula Field)	Ula Formation	Early Tithonian	Shoreface, offshore bar, tidal sand waves	(Ramm and Forsberg, 1991; Vollset and Dorê, 1984)

Table 3.1: Showing known common locations of Rhaxella Spicules (Tom Erik Mast, Thesis, 2008)

CHAPTER 4: METHODOLOGY

4.1. METHODOLOGY

This study has been divided in to two parts.

1) Well Correlation and Petrophysical evaluation
2) Petrographic Analysis using Optical Microscope and Scanning Electron Microscope (SEM)

Well information was gathered from Norwegian Directorate Fact Pages (NPD, 2011) and Petrobank. Three wells 2-1/6, 3-1/9-s, and 7-12/2 were investigated. Well 2-1/6 was the key well in the study and samples from cores of this well were studied only. Well 3-1/9-s and 7-12/2 were used only for correlation with 2-1/6.

4.2. WELL CORRELATION

The main objective of correlation was to correlate Ula Formation through Gyda, Tambar and Ula Fields. Ula Formation is divided into subparts on the basis of sequence stratigraphy and porosity (Ramm et al,. 1997). Correlation was done following this study and implementing it on the well 3-1/9-s. For correlation Gamma Ray log, Density log, and Neutron Porosity log were used. But other log types like Sonic log, Spontaneous Potential log were also used in combination.

Well correlation is totally based on sequence stratigraphic units recognized by Ramm et al., (1997). These sequence stratigraphic units were recognized on the basis of high and low porosity zones within the Ula Formation as they are stratigraphically correlatable throughout the Gyda, Tambar and Ula Fields.

Well correlation was done in Petrel. Petrel is a software introduced by Schlumberger. It can perform various operations like interpretation of seismic data, well correlation, and modeling of reservoirs. In this study only well correlation was performed. And for this purpose Petrel Version 2009 was used.

4.3. PETROPHYSICAL EVALUATION

Well correlation helped in recognizing low and high porosity zones. After correlation of the three wells, well log data of three wells was exported to Hampson and Russell. The Hampson-Russell

software suite encompasses all aspects of seismic exploration and reservoir characterization, from AVO analysis and inversion to 4D and multi component interpretation. For this study only E-log (component of software) was used to create cross plots. This made it possible to make different cross plots. e.g sonic- porosity vs density porosity color coded with gamma ray. This helped to match the recognized low and high porosity zones on the cross plots.

4.4. PETROGRAPHIC ANALYSIS

Petrographic analysis was done using Optical Microscope and Scanning Electron Microscope (SEM) on the samples taken from core material of well 2-1/6.

SEM analysis has been done on samples using JEO2 JSM-6460LV Scanning Electron Microscope (SEM) with a LINK INCA Energy 300 Energy Dispersive X-Ray (EDX) system. Two types of samples were studied under SEM. This includes thin sections coated with carbon and freshly fractured samples from core material which are mounted over stubs and coated with gold. 20 samples mounted over stubs were studied. And 10 samples were chosen for carbon coating in a way that it covered the high and low porosity zones.

Point Counting was also done using optical microscope on 20 thin sections from well 2-1/6. 300 points were counted on each thin section. It was done on Nikon Optiphot-Pol petrographic microscope in PPL (plain polarized light) and XPL (cross polarized light). Following parameters were determined.

1) Quartz 2) Feldspar 3) Rock Fragments 4) Matrix 5) Mica 6) Carbonate cement 7) Quartz cement 8) Primary Porosity 9) Authigenic Kaolinite 10) Illite 11) Secondary Porosity.

Point counting was carried out to get an overall idea of composition of samples and their porosity. Grain size distribution and sorting was also observed. Degree of sorting was estimated by following Longiaru (1987) (Figure 4.1). According to Longiaru (1987) sorting can be divided into Well, Moderate and Poorly sorted. An overview of which samples were observed from which depth is shown in the Table 4.1.

Data collected from Point Counting was used to calculate IGV (Inter granular volume). IGV is used to measure compaction in sandstones. IGV is equal to sum of intergranular space, intergranular cement, and depositional matrix (Paxton et al. 2002). IGV in sandstones is on average ranging from 40-45 volume percent (IGV at the time of deposition). IGV usually varies with sorting and particle grain size.

Well Name	Sample Name	Depth
2/1-6	2-12	4205.8
	2-14	4212.55
	2-15	4218.5
	2-16	4222.6
	2-17	4227.35
	2-18	4231.8
	2-19	4233.7
	2-21	4240.6
	3	4252.5
	4	4254.6
	5	4303.65
	6	4309.6
	7	4318.67
	9	4321.7
	10	4324.9
	11	4327.6
	12	4333.1
	13	4336.95
	14	4344.3
	16	4353

Table 4.1: Thin sections of the study area with their depths. Depths are measured in mRKB

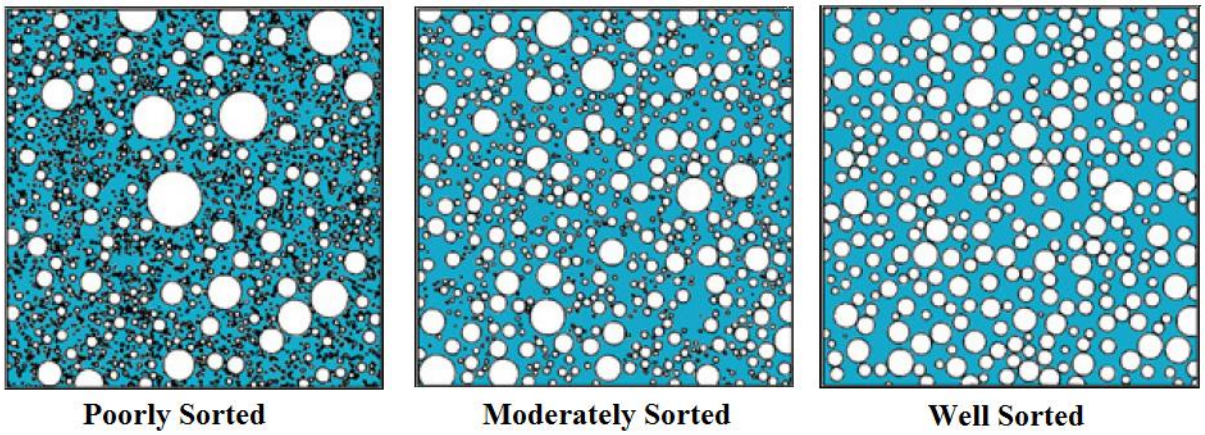

Figure 4.1: Degree of sorting presented by Choh et al, (2003) and modified after Longiaru, 1987..

CHAPTER 5: WELL CORRELATION AND PETROPHYSICAL DATA

5.1. INTRODUCTION

This chapter will focus on the investigation of petrophysical properties of the cored intervals in the study area. Data from well 1/3-9 S and 7/12-2 will not be petrophysically interpreted as this study focuses on the well 2/1-6 but these wells will be used for well correlation. The main purpose of well correlation and petrophysical study is to have knowledge of the lithology in the area and also mark the porous and non-porous zones in the cored intervals.

5.2. WELL CORRELATION

Well Correlation helps us in providing the lithostratigraphic framework for the cores and samples under study. Large amount of data can be derived from wire line logs but here these logs will be used to correlate the low and high porosity zones varying through the study area. Well correlation pattern was followed presented by Ramm et al, 1997 (Appendix A).

Figure 5.1 shows the well correlation followed by the interpretation of Ramm et al, 1997 and it is implemented on well 1/3-9 S as Ramm et al (1997) did not include this well in their correlation. Names of low and high porosity zones have been changed on purpose. Table 5.1 shows the name of these zones and the names used in this study.

Ramm et al. 1997	Current Study	Porosity
Unit A	Ula E	Low
Unit B	Ula D	High
Unit C 1 $_1$	Ula C	Low
Unit C 1 $_2$	Ula B	High
Unit C 1 $_4$	Ula A	Low

Table 5.1: Names and porosities of units of Ula formation recognized by Ramm et al. 1997 and in this study.

It should be noted that Ula B and C zones weren't recognized in well 7/12-2.

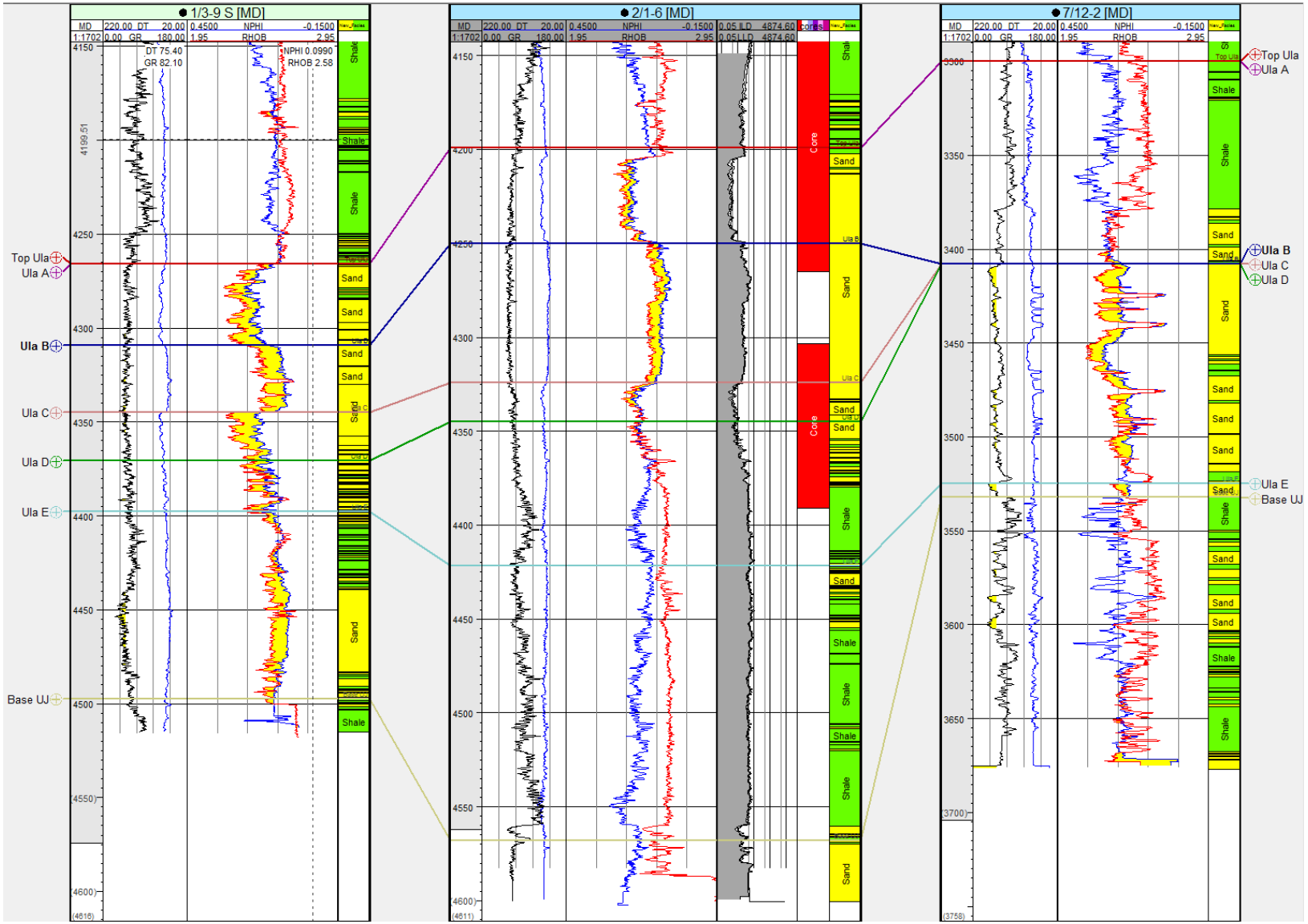

Figure 5.1: Well correlation of the 3 well from Tambar, Gyda, and Ula fields.

According to the table 5.1 there are only two zones Ula B and D which are high porosity zones. Ula A, C, and E are low porosity zones. Note that in Figure 5.1 in well 2/1-6 from depth 4200 mRKB to 4330 mRKB within a same sandstone unit we have three different types of porosity zones. Two are of very low porosity and one is of high porosity. Ula A and Ula C are of low porosity while Ula B is of high porosity as seen through the logs.

5.3. CROSS PLOTS

Various cross plots were made using Hampsson and Russel software by importing wire line log data. These crossplots are shown in Appendix E. Among all other crossplot P-wave against Density was the most useful because it indicates lithologies and porosities.

Figure 5.2 shows the cross plot between P-wave and Desnity color coded with Gamma Ray. Note that the High Porosity Sandstones have sonic wave velocities from 3700 to 4400 m/s with densities from 2.300 to 2.460. Low porosity sandstone have sonic wave velocities from 4500 to 5250 m/s with densities of 2.475 to 2.600. Also note that shales have very low densities and very low response to sonic wave velocity.

Figure 5.3 shows the same cross plot as Figure 5.2 color coded with depth. This cross plots shows all the low and high porosity zones of the data which was imported in Hamspon and Russell. From the color of the depth it should be noted that Ula B and Ula D fall in the category of High Porsoity Sandstones. Ula B ranges from 4250 m to 4325 m depth. While Ula D is at depth from 4345 m to 4421 m. Though high porosity zone of Ula D lies in the upper part which is only from 4345 m to depth of 4370 m. These depth ranges fall into the category of High Porosity Sandstones as shown in Figure 5.3. Ula A, Ula C and Ula E are sandstones with low porosity. Ula A is at depth of 4200 m to 4249 m. Ula C is at 4325 m to 4340 m depth. While Ula E ranges from 4420 m to 4565m depth. These depths fall in the category of Low Porosity Zones in the cross plot color coded with Vertical depth (Figure 5.3).

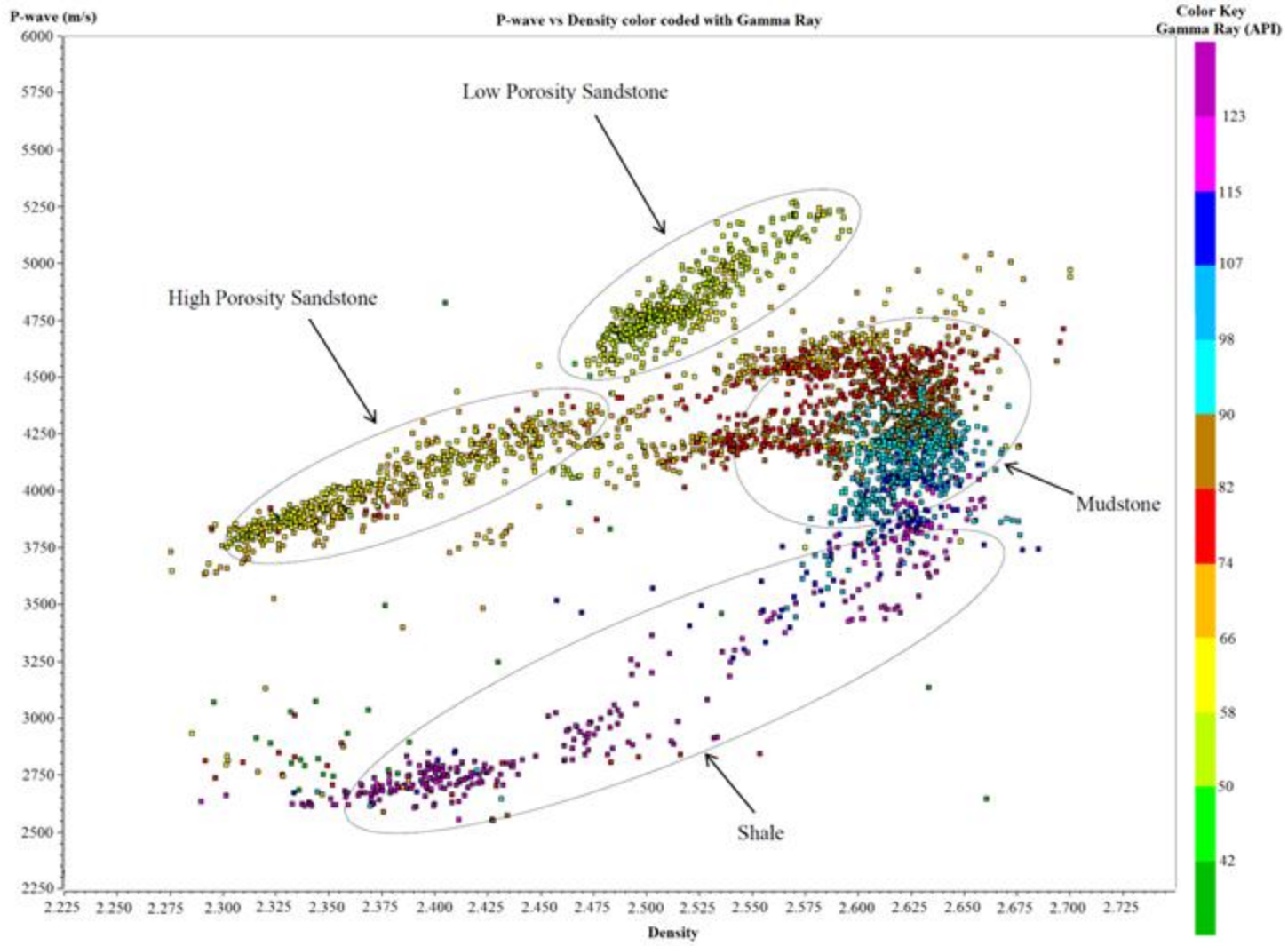

Figure 5.2: Cross plot of P-wave vs Density color coded with Gamma Ray.

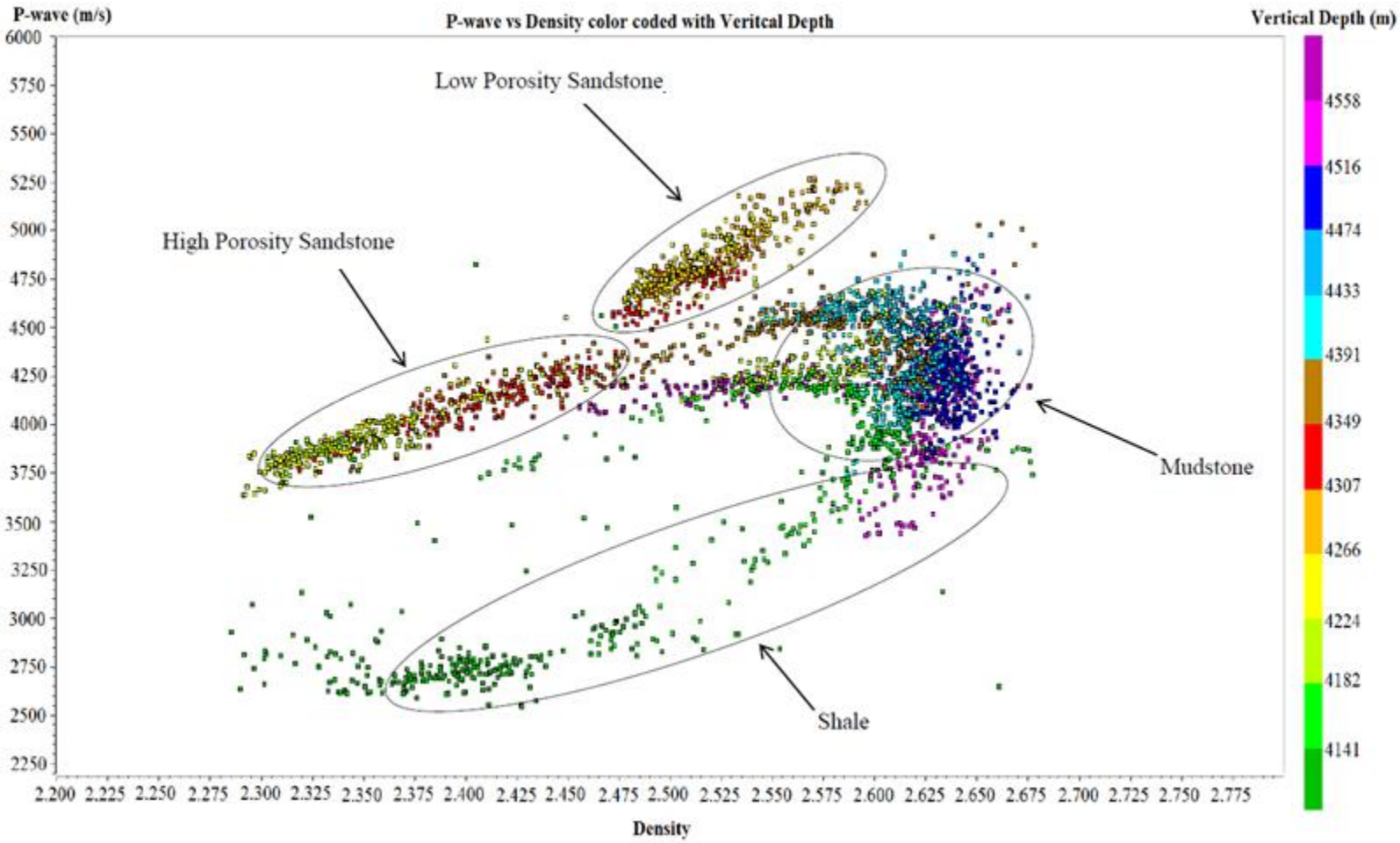

Figure 5.3: Cross Plot of P-wave vs Density color coded with Vertical Depth

CHAPTER 6: PETROGRAPHY

6.1. POINT COUNTING

Modal Analysis (300 points per sample) was performed on twenty different thin sections from well 2/1-6. The sampled sandstone from the well was predominantly sourced from the pre-rift sedimentary rocks that were uplifted in Late Jurassic time in the Central Graben. Therefore it was expected that sandstones would be mature (high quartz content). Point counting of the samples indicate that majority of the samples are Quartz Arenites and thereby confirms the compositional maturity that was expected. Five of the samples fall into the category of Subfeldspathic Arenites because of higher feldspar content (Figure 6.1). Results of the point counting are shown in Appendix C and in Table 6.1.

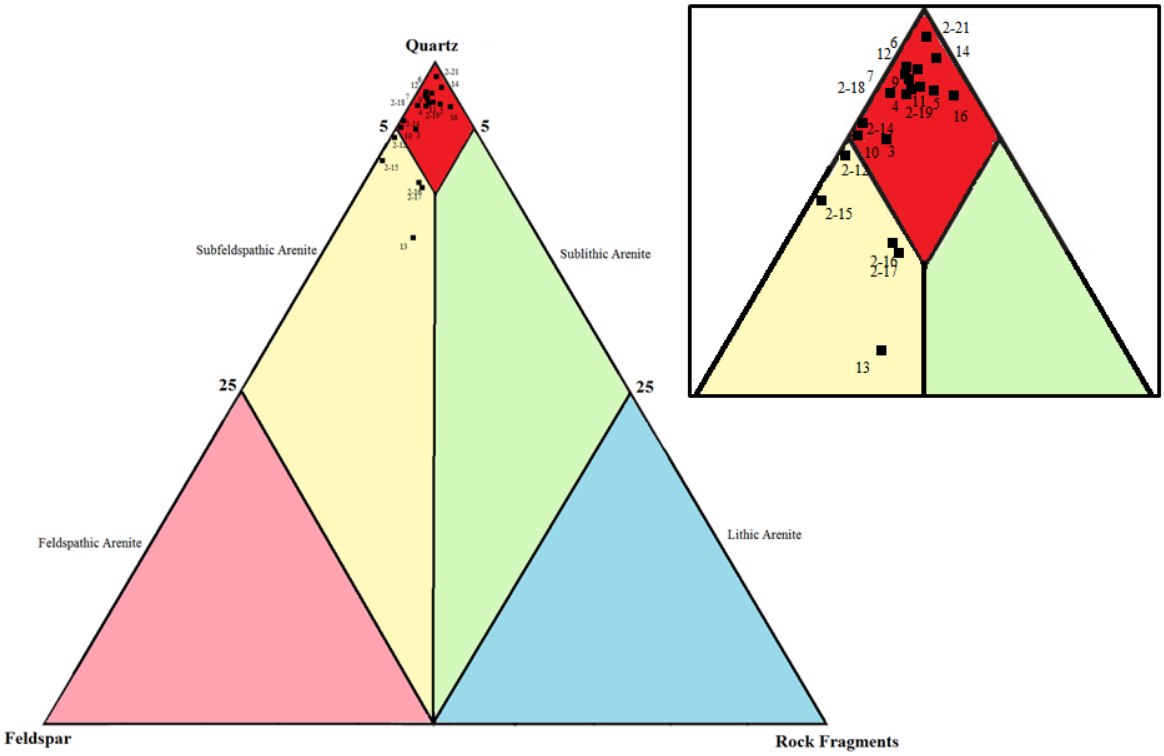

Figure 6.1: Classification of the samples following Pettijohn et al (1987). Box shows zoomed in data of plotted samples. Composition is also given in Table 6.1.

Sample	Depth (mRKB)	Avg Grain Size	Framework Composition			Matrix	Porosity	Quartz Cementation	Calcite Cementation
			Quartz	Feldspar	Rock Fragments				
2-12	4205.8	0.25	88.04	11.96	0.00	15.6	16.3	1.3	4
2-14	4212.55	0.0175	90.85	9.15	0.00	7.6	15	6.3	3.3
2-15	4218.5	0.0175	84.98	15.02	0.00	10.6	15	4.3	3
2-16	4222.6	0.015	87.85	12.15	0.00	15.3	15.6	3	4.3
2-17	4227.35	0.015	89.06	10.94	0.00	18	15.6	2	2.6
2-18	4231.8	0.0175	94.28	5.72	0.00	7	14.3	5	4
2-19	4233.7	0.01	91.72	8.28	0.00	8	14.3	1.6	3
2-21	4240.6	0.02	93.94	6.06	0.00	6	13.3	1	1.3
3	4252.5	0.02	88.04	11.54	0.42	6.3	9.6	4.6	5.3
4	4254.6	0.025	94.31	4.94	0.74	2.3	5	3.3	3
5	4303.65	0.255	91.11	8.89	0.00	9.6	8.6	5	1.6
6	4309.6	0.2525	94.18	5.82	0.00	9.6	5.3	4	4.6
7	4318.67	0.0175	95.36	4.64	0.00	8	4.3	2.6	3.3
9	4321.7	0.25	94.79	5.21	0.00	19	15	2.6	0.6
10	4324.9	0.0175	91.44	8.56	0.00	11.3	9.3	4.3	1.6
11	4327.6	0.02	95.41	4.06	0.53	22.3	12.3	4	2.6
12	4333.1	0.015	96.45	3.55	0.00	17.3	11.3	4	6
13	4336.95	0.0125	85.53	14.47	0.00	18.3	17.6	2	2.6
14	4344.3	0.0125	97.15	2.85	0.00	14	14.3	1.3	6.3
16	4353	0.0125	92.74	6.65	0.60	29.3	7.3	2.3	5.3

Table 6.1: Results of petrographic analysis.

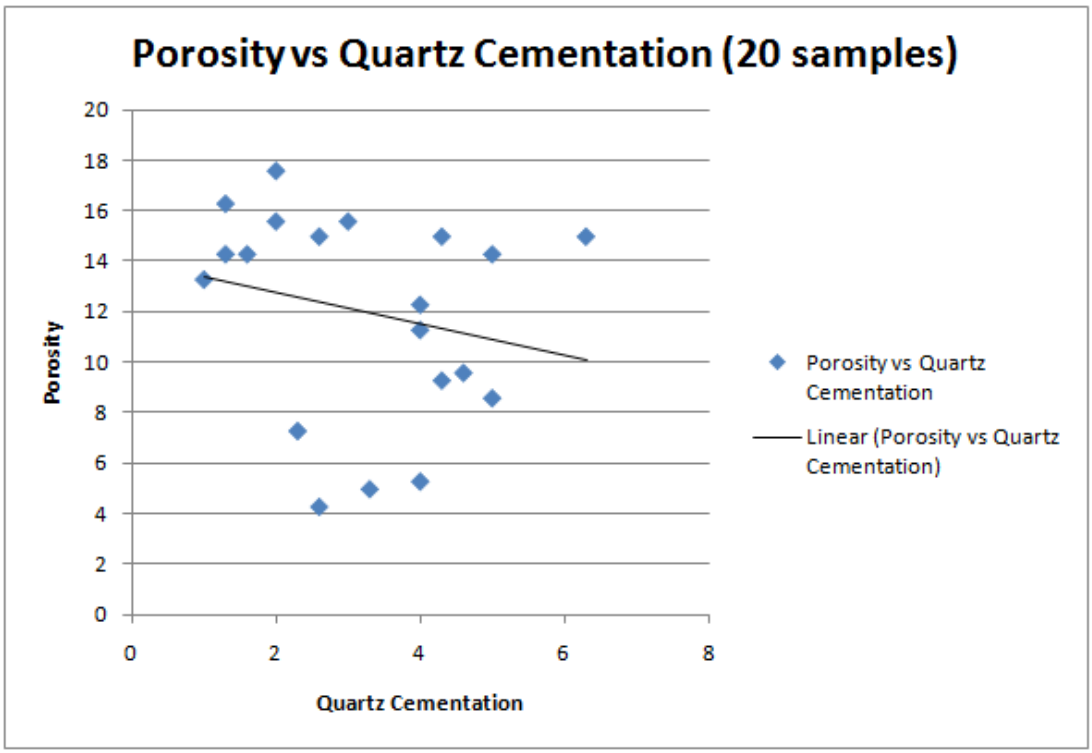

Figure 6.2: Cross plot of Porosity vs Quartz cementation.

Figure 6.2 shows the cross plot showing a relationship between Porosity and Quartz Cementation. From this cross plots it should be noted that porosity decreases with increasing cementation. And it's clearly indicated by this cross plot that there is a linear relationship between porosity and quartz cementation. If porosity is high, quartz cementation is low and if quartz cementation is high porosity is low.

Thin sections from well 2/1-6 were grouped semi-qualitatively visually in the microscope according to the degree of sorting as poor, moderate or well sorted as shown in Appendix B. Most of the samples are well sorted. It should be noted that samples with low porosity at log are sub-angular to angular and are moderately to well sorted. While high log porosity samples are sub-rounded and are mostly moderately sorted indicating that both compositionally and texturally they are mature. Though there are a few poorly sorted samples with high log porosity.

6.2. IGV

Inter Granular Volume (IGV) was calculated and is presented in the Figure 6.3. The average IGV of the well 2/1-6 is 31.5% and range between 14% to 44%. We get the minimum of IGV in sample 4 at depth of 4254.6 m depth. Reason for low IGV in this sample is this that it is compacted and has very low matrix content. The highest IGV is 44% at depth of 4353 m. Reason for high IGV is large amount of matrix as observed in thin section. Most of the samples have IGV above 30%. The reason for high IGV in most of the samples is high matrix content.

Cross plot of IGV vs Matrix was also created (Figure 6.4). This cross plots clearly shows that we have a very nice correlation between IGV and the Matrix. Where we have high matrix we have higher percentage of IGV. Similarly, where we have low amount of matrix we have low percentage of IGV.

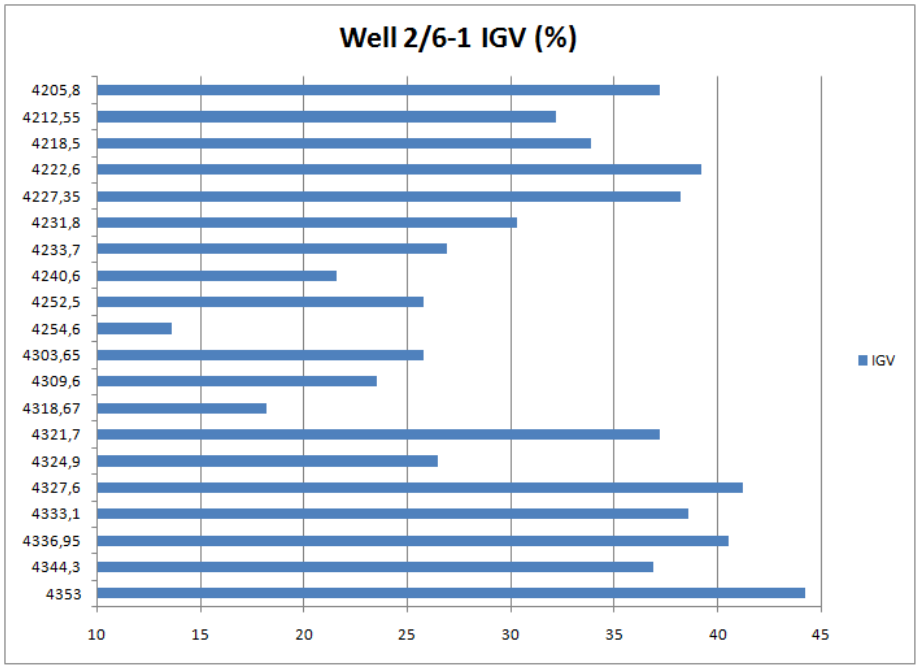

Figure 6.3: Inter Granular Volume from well 2/1-6. IGV is on X-axis and depth is on Y-axis. It shows variation in IGV with depth.

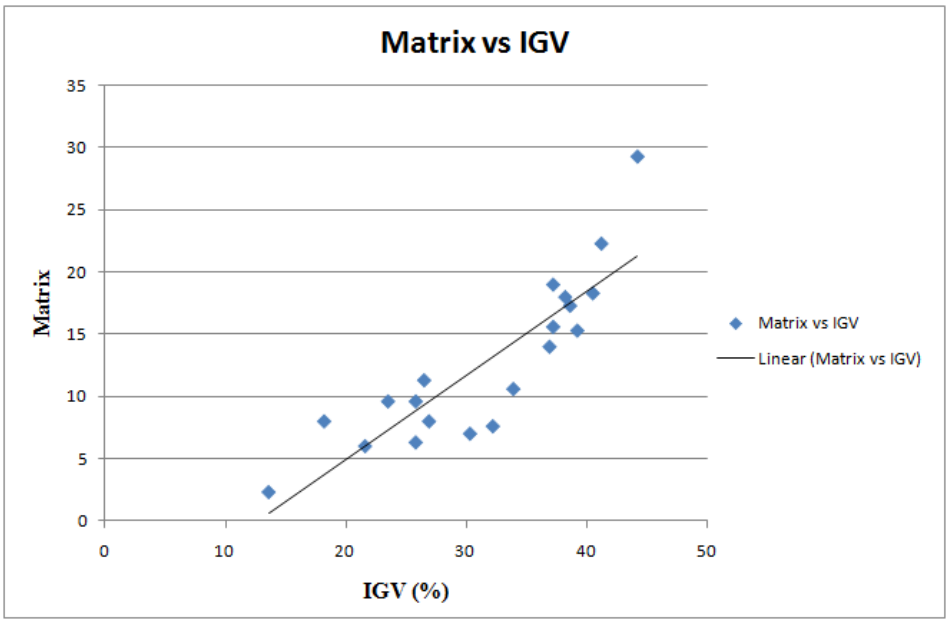

Figure 6.4: Cross plot of IGV against Matrix.

6.3. SEM

Twenty samples, from well 2/1-6 of both well cemented and poorly cemented sandstones, have been examined under SEM. Purpose of study of samples under SEM was to identify grain coatings, mineral associations and quartz overgrowth. Grain coatings which were recognized were micro-quartz, illite, chlorite grain coats. Smectite was not recognized in the samples. All minerals identified in study were identified by Energy Dispersive Spectrometer (EDS). A wide range of minerals have been identified which include: quartz, feldspar, illite, chlorite, apatite, mica, calcite, dolomite, ankerite. Backscatter Image and Cathode Ray Iluminesence were used together to identify the quartz overgrowth.

6.3.1. RESULTS

Almost all of the samples studied under SEM had some degree of grain coats. Two figures will be presented to give an introduction to the petrographic results by SEM. Figure 6.5 gives typical examples of micro-quartz and clay coats present in the study area. Figure 6.6 illustrates that how grain coats have prevented quartz grains to grow and have preserved the reservoir qualities.

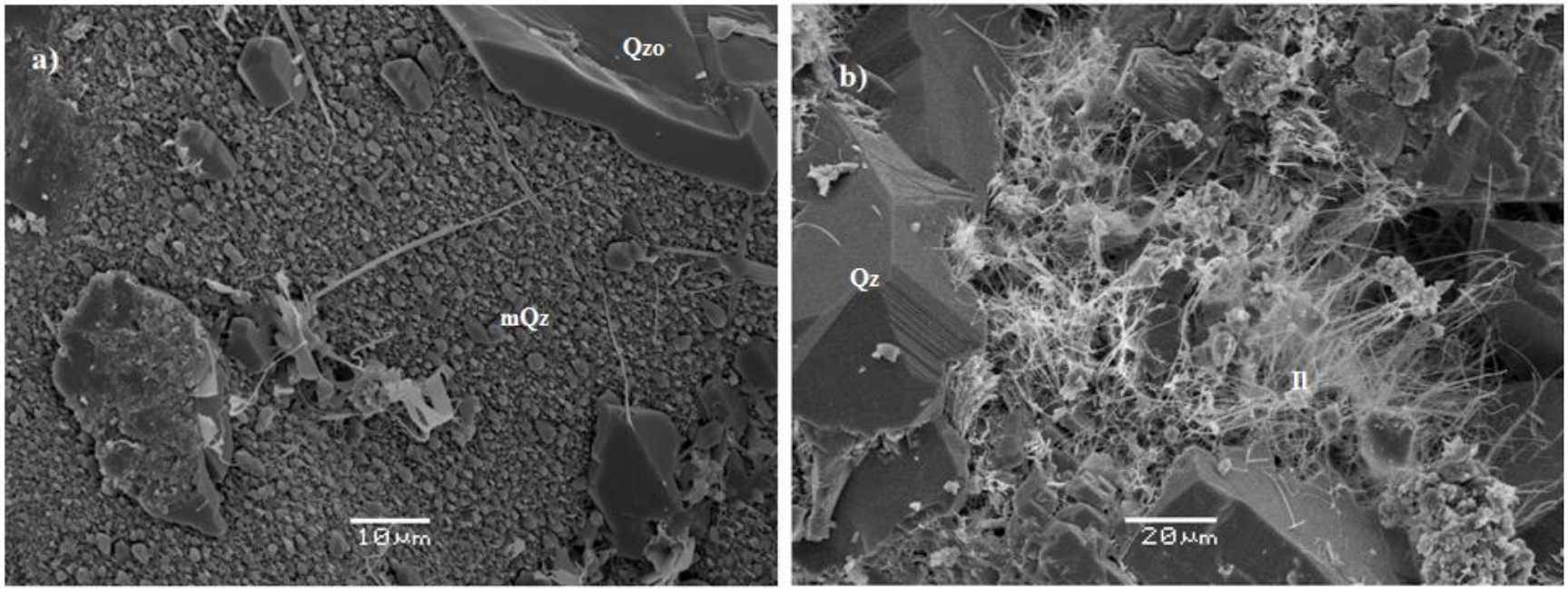

Figure 6.5: Showing typical examples of grain coats like micro-quartz (mQz) and illite (Il) present in study area. Quartz overgrowth (Qzo) can be seen in a. Quartz cementation over quartz grain can be seen in b. Picture (a) was taken from sample 11 and (b) was taken from sample 3.

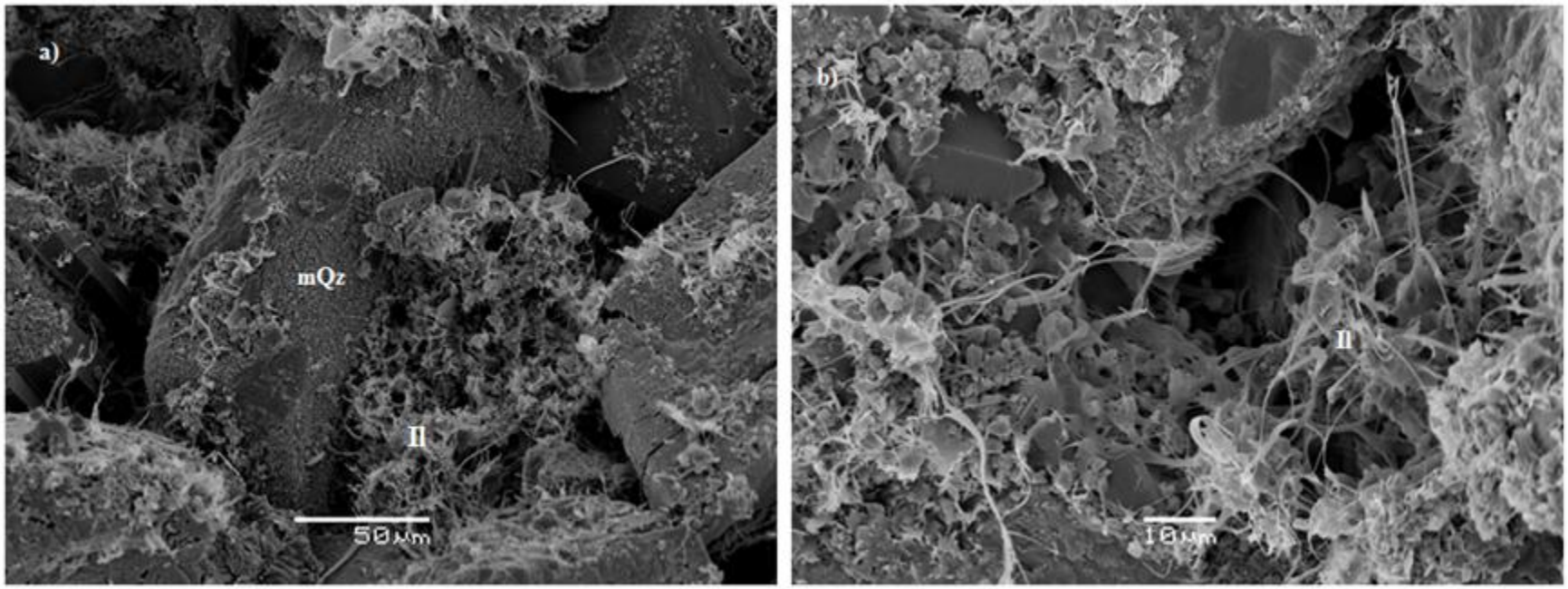

Figure 6.6: Showing preservation of porosity in sandstones by the grain coats. Micro-quartz (mQz) and Illite (Il) are covering whole quartz grain in (a). Fibrous pore filling Illite (Il) in(b). Picture (a) was taken from sample 11 and picture (b) was taken from sample 12.

6.3.2. GRAIN COATS

Micro-quartz is the main grain coat observed in almost all of the samples (Figure 6.7). Micro-quartz grain size in studied samples is usually 0.5 to 2 μm in size (Figure 6.8). Various amounts and developments of macrocryastlline quartz overgrowths with the detrital quartz were also recorded (Figure 6.7, 6.8). Micro-quartz grain coating is usually extensive covering all the surface of grains. But where it is not covering the whole grain, could not stop quartz overgrowth and destroying the reservoir qualities. Sponge spicules e.g Rhaxella, were also observed in samples 2-15, 2-18, 4, and 5 (Figure 6.9, 6.10).

Clay coats were also observed in these samples. Illite was the most common clay frequently observed clay coat. Chlorite clay coat was rarely found in the samples (Figure 6.12 and 6.13). Chlorite clay also shows honeycomb morphology as observed in Figures 6.12 and 6.13. Clay coats were mostly found in combination with micro-quartz grain coating (Figure 6.14 and 6.15) but also were observed where no micro-quartz was present (Figure 6.16). Though clay grain coats were present in the observed samples but micro-quartz was the most common observed grain coat which resulted in preservation of good reservoir qualities.

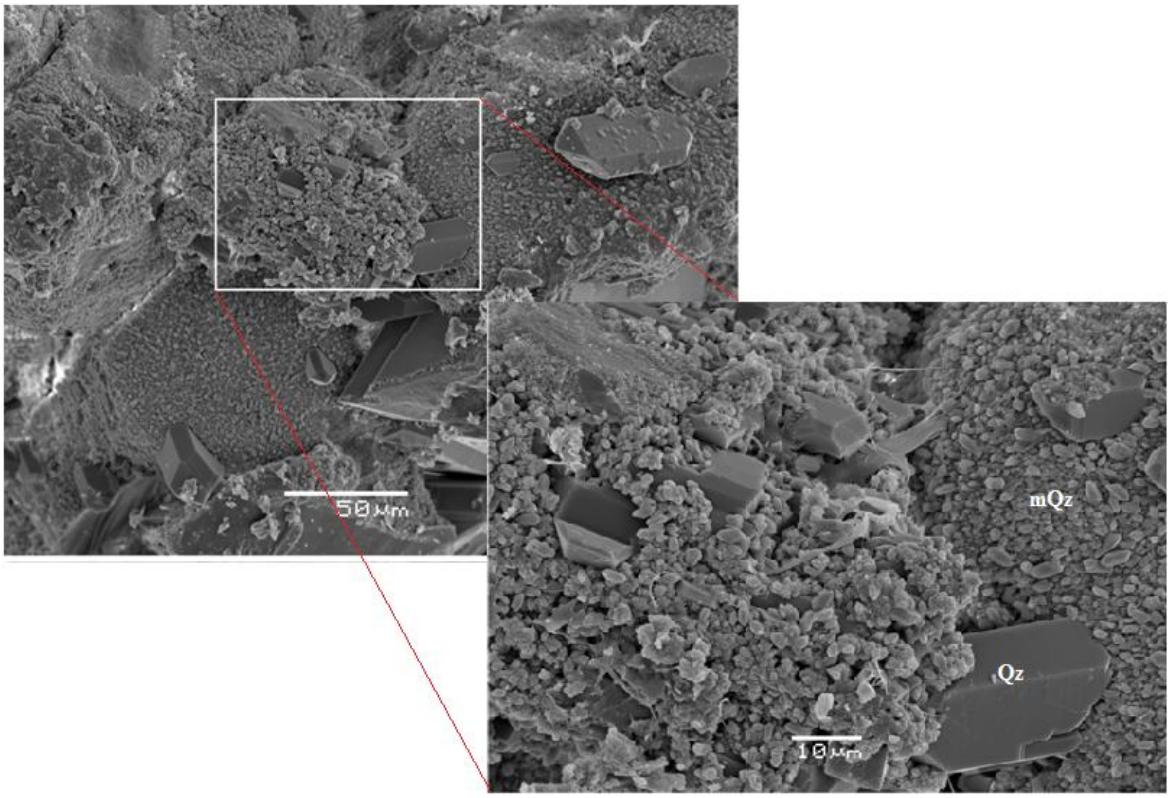

Figure 6.7: Showing extensive micro-quartz (mQz) coating over quartz grain with quartz overgrowth over it. Picture was taken from Sample 2-17.

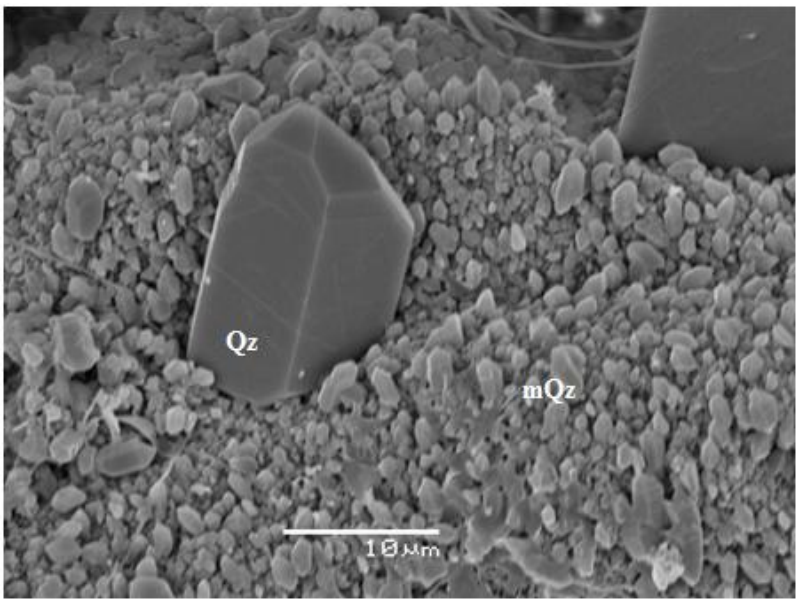

Figure 6.8: Showing micro-quartz grain coating (mQz) and size variation of micro-quartz grains. Overgrowth (Qz) of euhedral quartz grain within the micro-quartz grain coating probably because grain coat didn't cover all of the grain. Picture taken from sample 2-18.

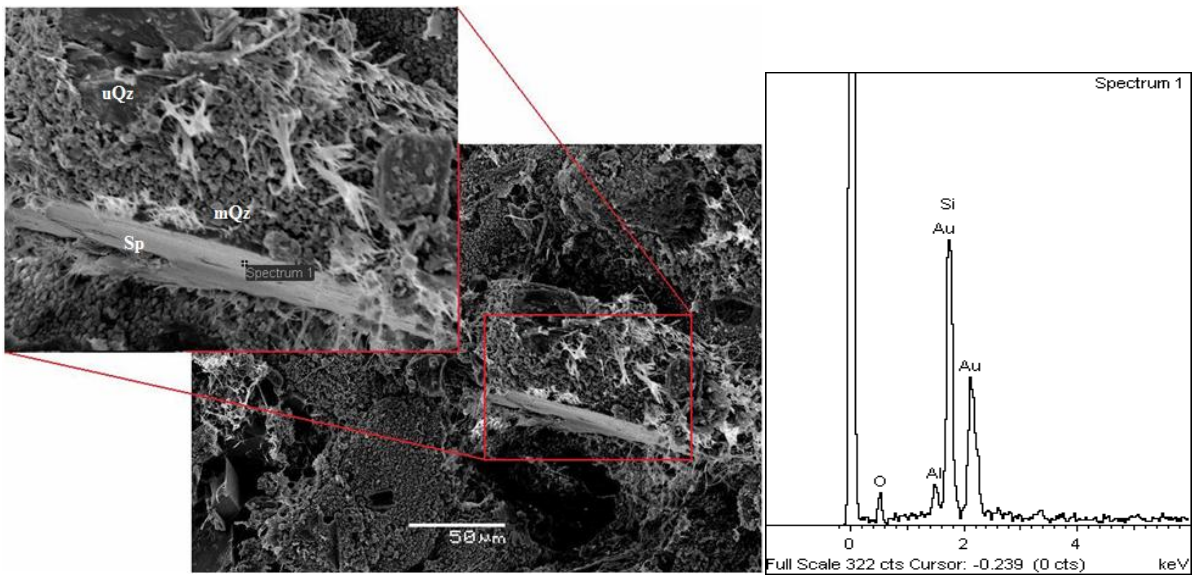

Figure 6.9: Showing sponge spicule (Sp) lying over a quartz grain coated with micro-quartz (mQz) grain coating. . Uncoated surface (uQz) of quartz grain is also visible. EDX spectrum showing peaks of Silica and Oxygen at sponge spicule. Picture taken from sample 2-15.

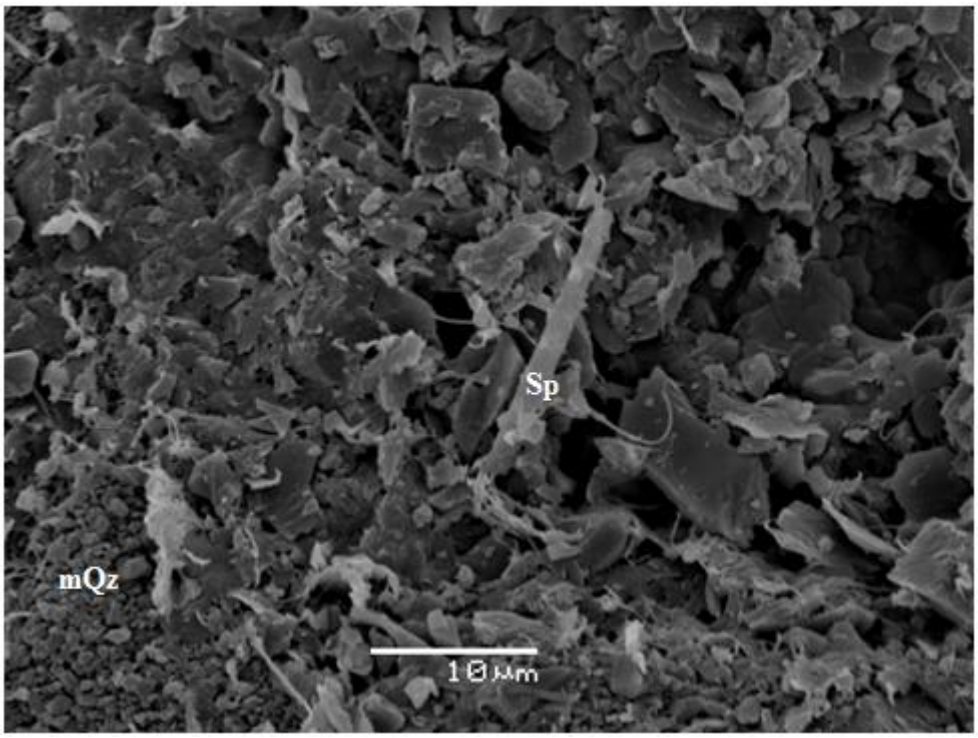

Figure 6.10: Showing sponge spicule (Sp) and micro-quartz (mQz) on one side. Picture is taken from sample 5.

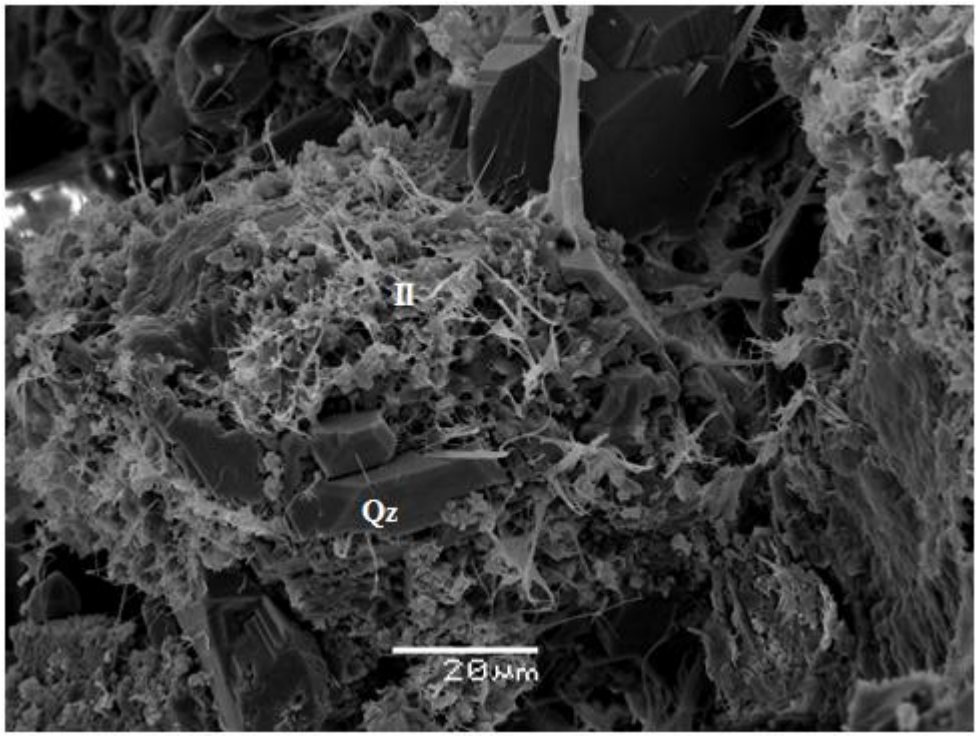

Figure 6.11: Pore filling Illite (Il) layer over quartz grain with quartz overgrowth (Qz). This picture is taken from sample 2-21.

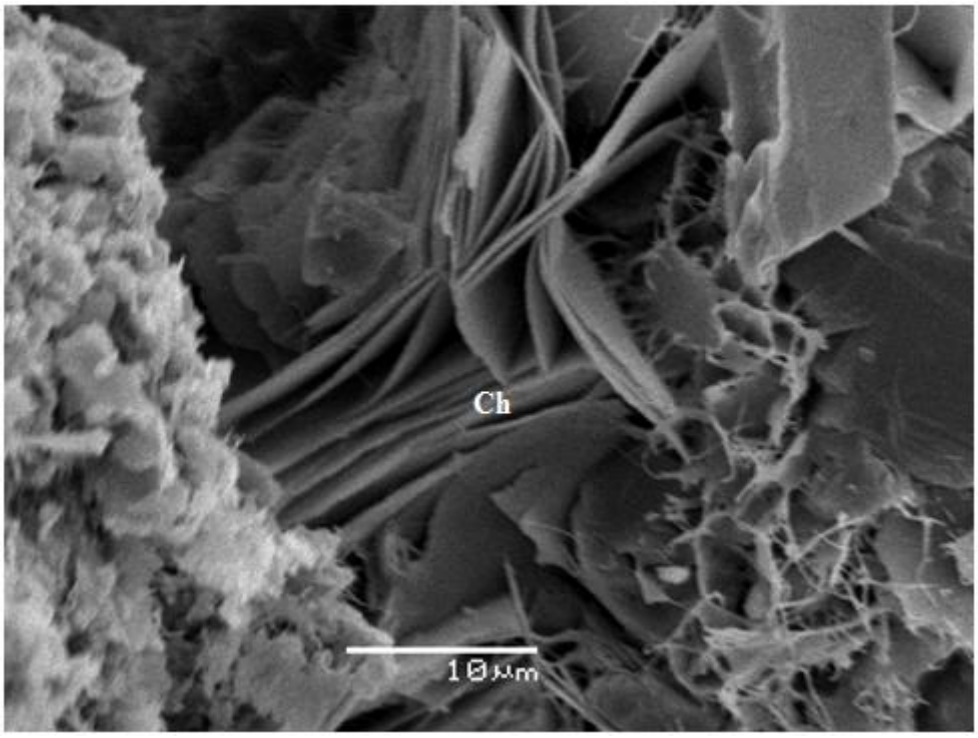

Figure 6.12: Showing chlorite clay (Ch). This picture is taken from sample 3.

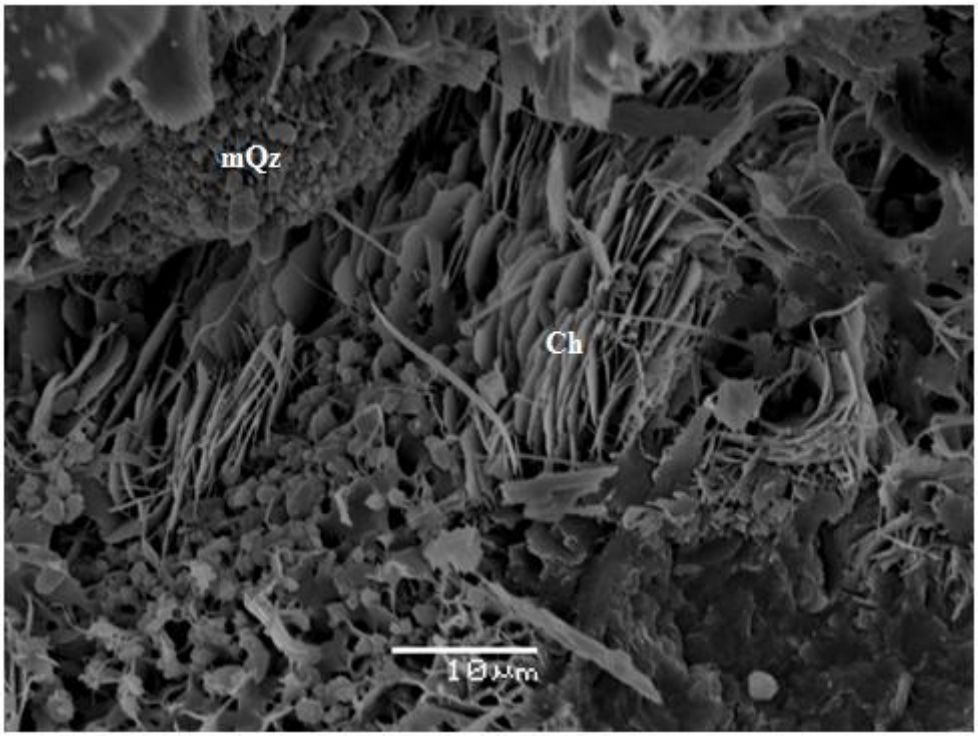

Figure 6.13: Pore filling Chlorite clay (Ch) showing its characteristic honey comb morphology. Micro-quartz (mQz) is also covering another quartz grain. This picture is taken from sample 11.

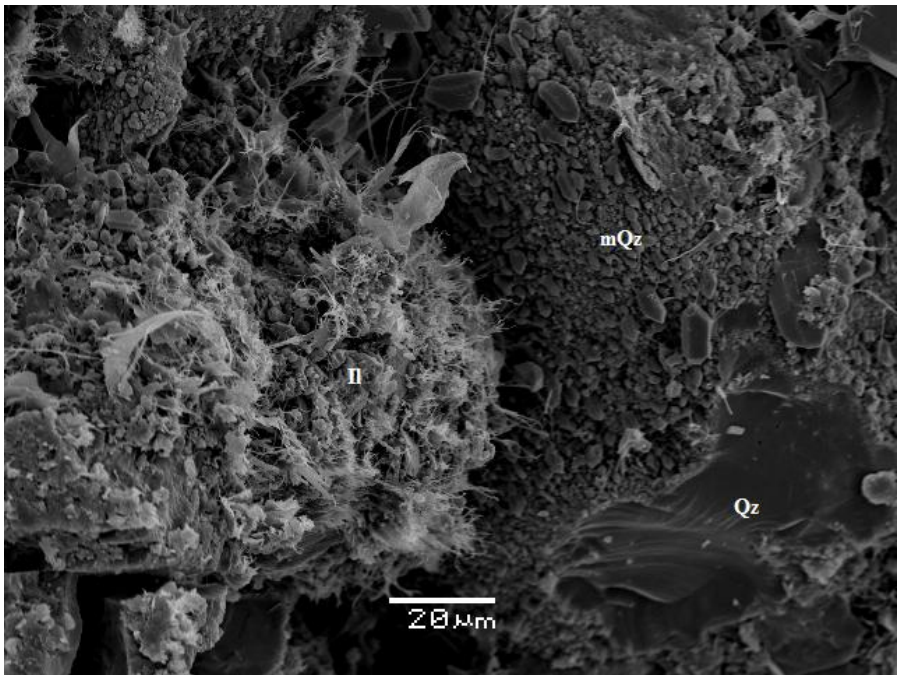

Figure 6.14: Illite clay (Il) extensively covering the whole grain and micro-quartz (mqz) covering part of other grain. Quartz overgrowth (Qz) where no grain coating is present. This picture was taken from sample 9.

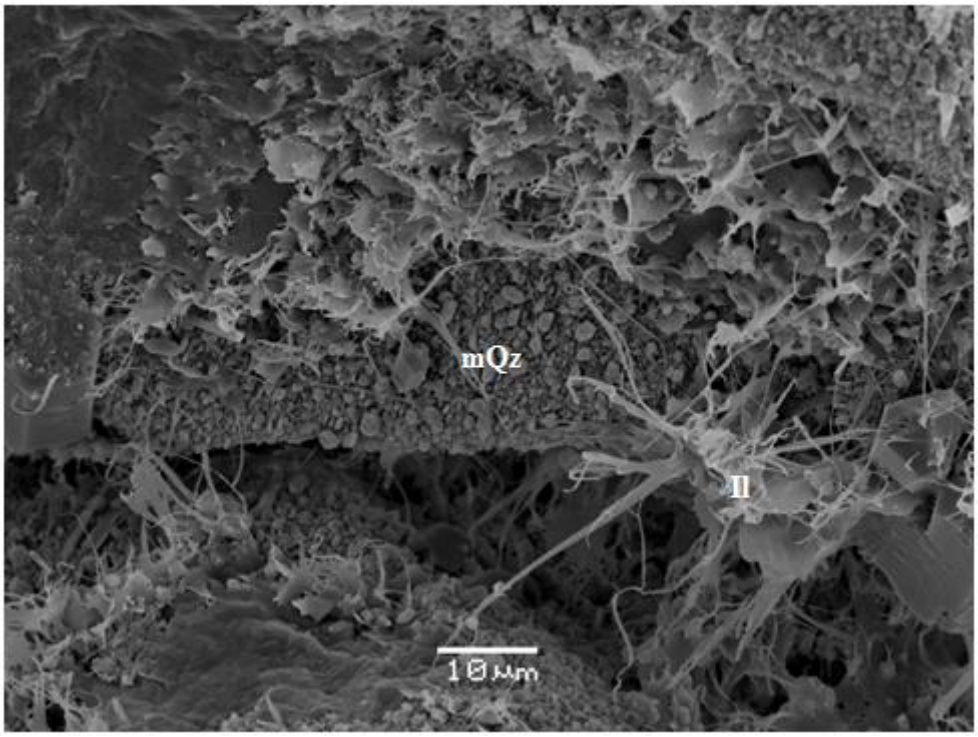

Figure 6.15: Pore filling fibrous Illite clay (Il) and micro-quartz (mQz) covering the whole grain extensively. This picture was taken from sample 11.

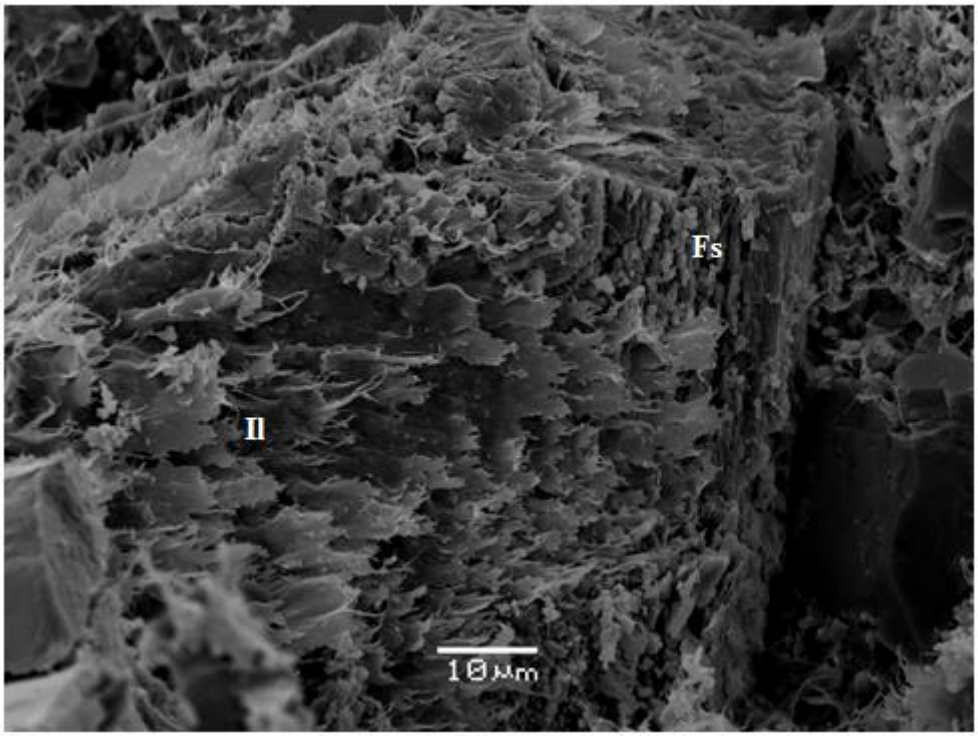

Figure 6.16: Showing Illite (Il) grain coating over K-feldspar (Fs) grain. No micro-quartz is seen around the grain. This picture was taken from sample 2-21.

6.3.3. QUARTZ OVERGROWTH

Quartz grain overgrows where grain coats like micro-quartz and clay coats are absent. Quartz overgrows through spiral-growth. In Figure 6.17 it is clearly visible that all of the porosity is lost by quartz overgrowth in the pore space. In the middle there is mica with sheet of illite in between its flakes. Quartz overgrowth can also be seen using Back Scatter Image and Cathode Ray Iluminesence together. In Figure 6.18 note that comparison of two pictures show that quartz grain was deposited in a sub angular shape (a-2) while later it was connected with other quartz grain by quartz cementation (a-1). Similarly in Figure 6.18 b-1 and b-2, it is clearly visible that quartz cementation and overgrowth have reduced the porosity and in turn destroying the reservoir quality.

Overgrowth was also observed in the form of a number of prismatic crystals (Figure 6.19) which grow on detrital quartz covered with micro-quartz. As grain coats like micro-quartz covers the grain, the overgrowth of detrital quartz grain stops. But as silica saturations rises to higher level, micro-quartz grain start to overgrow. This is shown in Figure 6.19. Note that small crystals of micro-quartz have overgrown in to a bigger size of quartz crystals. In this figure also note that quartz over growth has occurred where micro-quartz has not covered the grain.

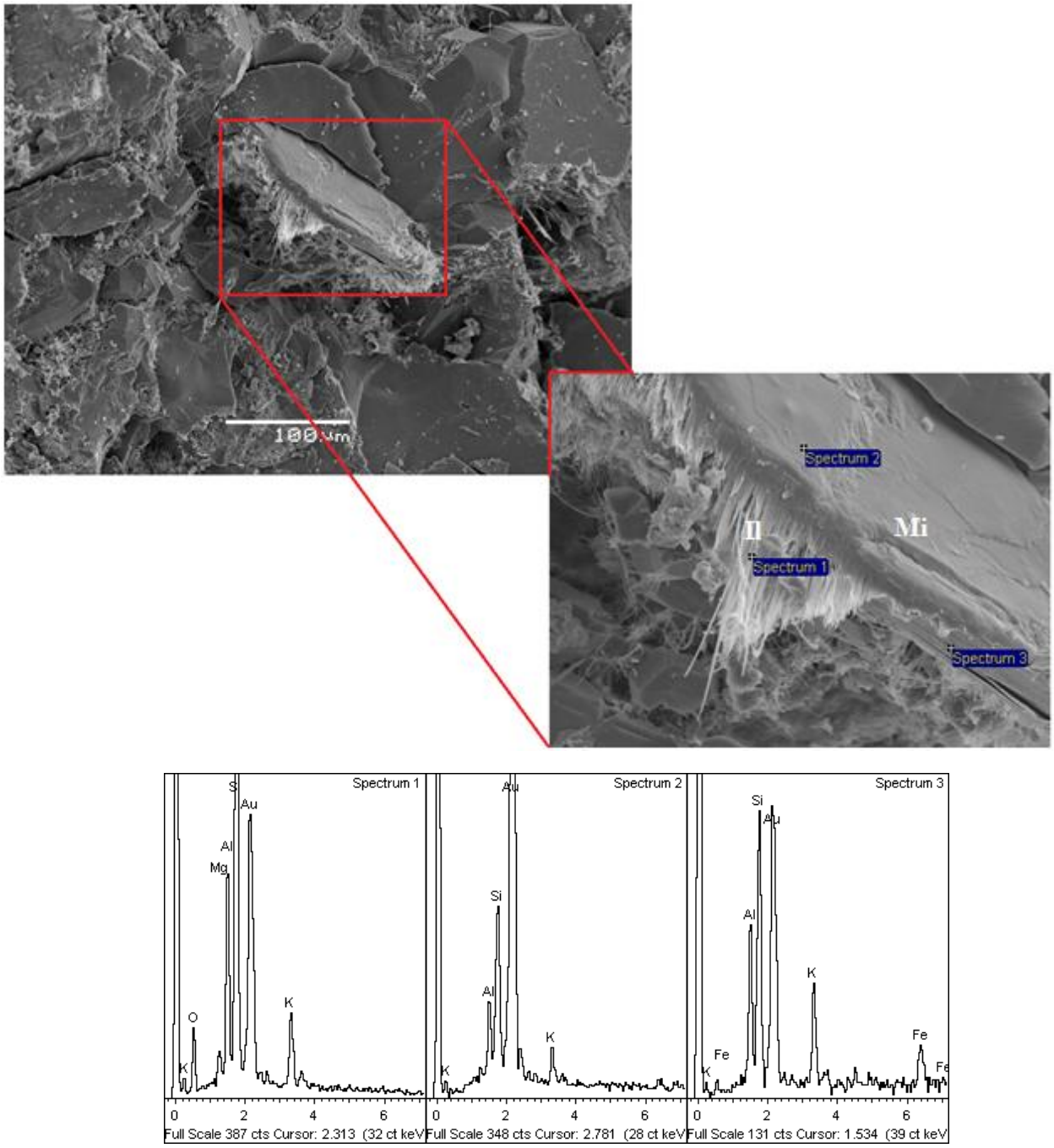

Figure 6.17: Typical spiral quartz overgrowth pattern in absence of grain coats. Il= Mica, Il= Illite clay. Spectrum 1= Illite, Spectrum 2= Mica, Spectrum 3= mica. (picture taken from sample 3).

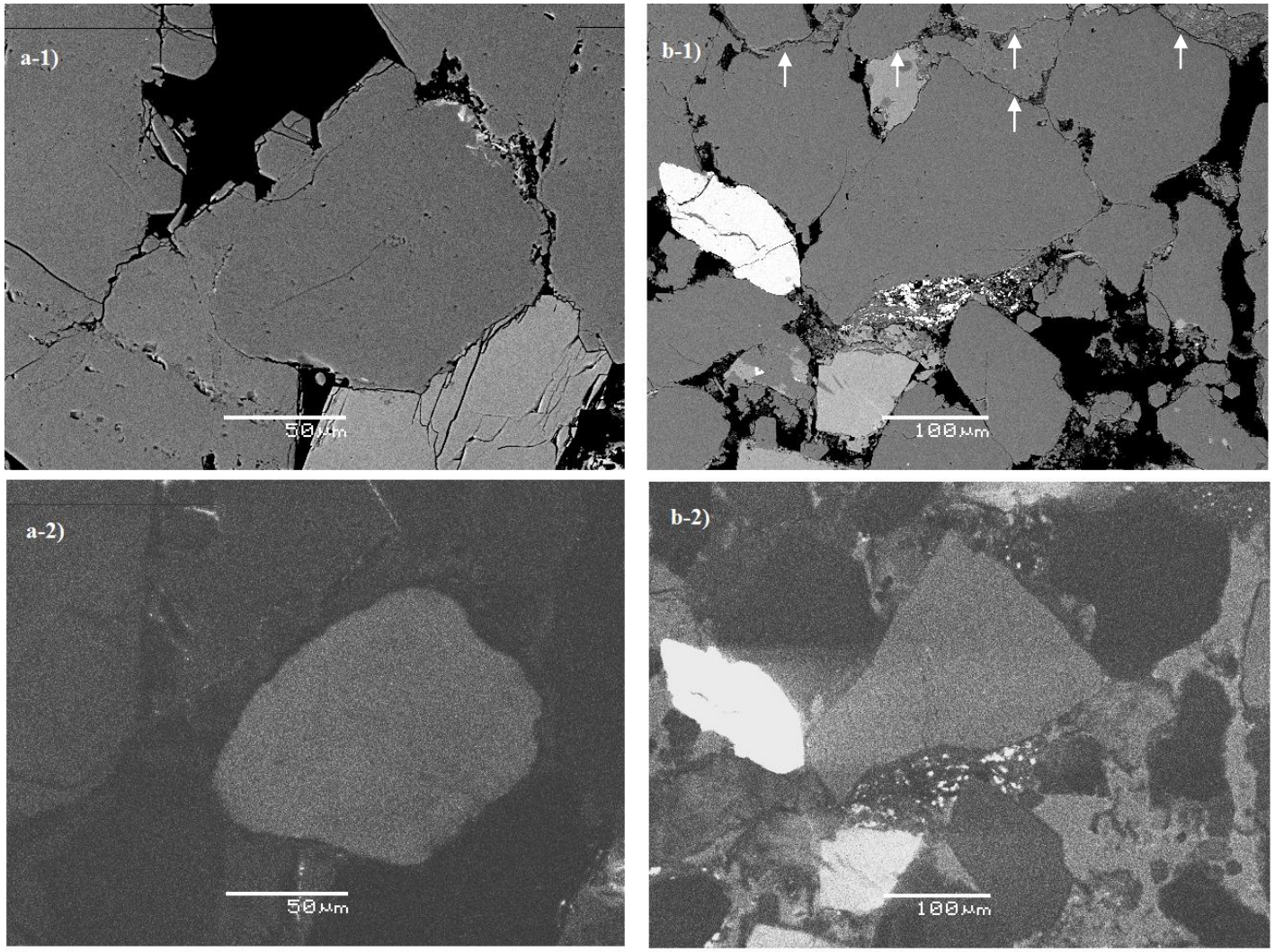

Figure 6.18: Showing quartz cementation over a quartz grains destroying reservoir quality. Grain crushing in a-1) is also visible. a-1) and b-1) are backscatter images. (a-2) and (b-2) are Cathode Ray Illuminesence images. White arrows on (b-1) marks the stylolites (picture was taken from samples 2-16 and sample 2-19).

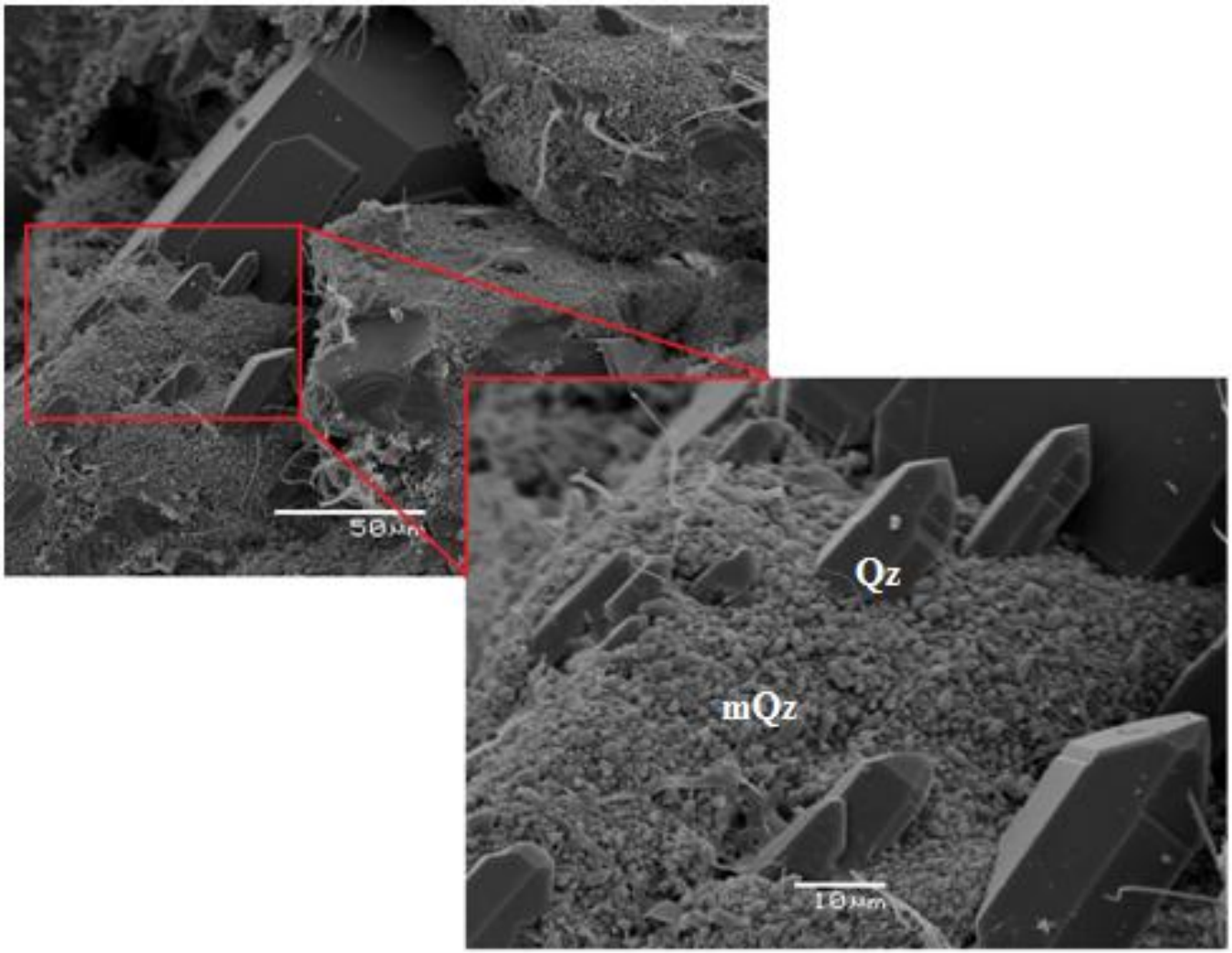

Figure 6.19: Showing overgrowth of micro-quartz grains due to high saturation of silica. mQz= Micro-quartz, Qz= Quartz overgrowth (picture was taken from sample 2-12)

7. DISCUSSION

7.1. INTRODUCTION

From the last two chapters it has been shown that grain coatings like micro-quartz and clay coats are present in the area and are of primary importance in preserving porosities at depths of greater than 4 km. From the results it has also been suspected that grain size and shape has also played an important role in preserving porosities.

As Ula Formation is divided in zones based on high and low porosities. Five zones were recognized including Ula A, B, C, D and E. Only samples from Ula A, B, C and D were studied. Ula B and upper part of Ula D are the zone with high porosity while other zones are of very low porosity. As micro-quartz grain coating is present in all samples, so the reasons should be discussed that why porosities in Ula A, C and lower part of D were not preserve.

7.2. EFFECT OF MICRO-QUARTZ GRAIN COATS ON RESERVOIR QUALITY

SEM results (Chapter 5) show that grain coating micro-quartz is present in all of the twenty samples in study. North Sea is well known for presence of micro-quartz grain coating in the Jurassic sandstone reservoirs. As discussed in chapter 3, micro-quartz grain coats are the major reason of preservation of high porosities at depth greater than 4 km in the upper Jurassic sandstones of the North Sea. But from the results (Chapter 5) it is found that Ula Formation has zones with high and low porosities despite the fact that all of the samples have micro-quartz grain coating in them. Ula B and upper part of Ula D are the zones with high porosity while Ula A and Ula C are low porosity zones (Figure 5.1, Appendix C). From all these zones micro-quartz coating was recorded. Reason for high porosity in Ula B is obvious that micro-quartz preserved the porosity. But here question arises that what caused the Ula A and C to have low porosities? Reason for low porosity could be related to the grain size and grain shape. Samples from Ula B are mainly of medium grain size and sub-rounded while samples from Ula A and C are fine grained and angular sandstones (Appendix B). Fawad et al. (2011) reported that when angular grains are subjected to medium and high stress conditions they show increased porosity reduction. As in angular sand grains contact forces are more concentrated because there are very small contact areas as compared to rounded grains. This caused the grain crushing and increase in porosity loss in Ula A and Ula C. Reason for preservation of porosity besides micro-quartz

grain coating in Ula B can be the sub-rounded shape of sand grains. As the area of contacts in sub-rounded grains is higher and it causes the sands to sustain more compaction at greater depth (Chuhan et al. 2003).

The presence of micro-quartz grain coatings indicates that an amorphous silica precursor was present earlier in the sedimentary/diagenetic history of the sandstone (Maliva & Siever, 1988). These silica precursors are most likely sponge spicules as shown in Figure 6.9, 6.10. Micro-quartz coat is caused by transformation of siliceous sponge spicules known as Rhaxella Perforata (Ramm & Forsberg, 1991, Aase et al, 1996, Hendry and Trewin, 1995). Thus, micro-quartz occurrence totally depends on the sedimentary environment and sediment age.

Few sponge spicules or remnants of it were observed in the studied samples. This is in accordance with Vagle et al. (1994) who observed that sponge spicules were subjected to rapid decomposition. So, before deposition spicules were reworked because of decomposition. But Rhaxella spicules and micro-quartz together are reported from a wide variety of depositional environments which indicates that spicules were transported in those settings by sedimentary reworking (wave processes, tidal processes, gravity transport). So, it is difficult to interpret the specific settings in which Rhaxella Perforata is to be found but it seems that there presence is always linked shallow marine environment (Table 3.1).

7.3. Effect of Clay Coats on Reservoir Quality

Results show that the most common and frequent clay mineral (grain coat) found in twenty samples is Illite. Illite was also observed with chlorite clay grain coating. According to Bjørlykke and Aagaard (1992) the most common clay mineral observed in the study area is Illite. Two diagenetic processes can lead in the formation of illite in the reservoir, either by illitization of kaolinite or from a smectite precursor (Bjørlykke and Aagaard, 1992). Morphology of illite supports the second diagenetic process as the main cause of Illite grain coating in the study area. Smectite was not observed in the samples as smectite is only stable till 70°C. And all twenty samples are at depth greater than 4 km with temperatures of about 140 to 150°C. After 70°C, smectite converts into illite or chlorite. Chlorite clay coatings were minor but wherever they are

present they show honeycomb morphology (Figure 6.12, 6.13) which indicates that the coatings have a possible smectitic precursor.

Micro-quartz is the most abundant and usually present grain coat in the studied samples and that is the reason that affect of illite coats on porosity has been hard to be estimated. These clay coats are usually thin and therefore may not compete with micro-quartz in preserving reservoir porosity even if clay coats were abundant. That is the reason that in study area, illite and chlorite are considered as the secondary contributor in the preservation of porosity by inhibiting quartz cementation. Moreover, illite coats could be of more importance locally.

7.4. QUARTZ CEMENTATION

Quartz cement in samples of well 2/6-1 ranges between 1 to 6.3% (Figure 6.2, Appendix C). Majority of the samples have less than 4% quartz cementation. Samples which have ≥ 4% quartz cementation are generally fine grained (Appendix C) which implies that large surface area promotes quartz cementation. Scanning Electron Images (Figure 6.17) show that quartz cementation grown in to the pore space and destroys the porosity until or unless grain is covered by some grain coating like micro-quartz or clay coats. Quartz overgrowth was recognized easily by comparing backscatter images and CL images. CL images easily differentiate between detrital quartz grain and quartz overgrowth caused by cementation around it (Figure 6.18) (e.g Götze et al. (2001)). Quartz overgrows through spiral growth. But this type of overgrowth was not observed in the studied samples. Though, normal quartz overgrowth was observed as shown in Figure 6.17. This type of quartz overgrowth is caused by low (<5%) silica saturations (Jahren and Ramm, 2000). Source of quartz cement in Ula formation can be a pressure-solution along stylolites. Contacts between illite clay or mica and quartz grain are the preferred sites of dissolution. These contacts are called stylolites (Fisher et al., 2000).

7.5. RESERVOIR QUALITY: A REGIONAL SCALE PERSPECTIVE

Three different wells from Ula, Gyda, and Tambar fields were correlated on the basis of porosity variation trends in the area (Figure 5.1). Well correlation was done by following studies done by Ramm et al (1997) (Appendix A). High porosity zones recognized in the study are Ula B and upper part of Ula D. While low porosity zones are Ula A, Ula C and Ula E. Figure 5.1 shows that

the most important and high porosity sandstone Ula B is easily correlateable in Gyda and Tambar Fields but it is not present in Ula Field. In well 7/12-2 (Ula Field) we have only one high porous zone which is the upper part of Ula D. Ula A and Ula E are low porosity zones. Ula C is also absent in well 7/12-2. From the correlation (Figure 5.1), we can say that porosity preservation mechanisms in the Tambar and Ula Fields are the same as in Gyda Field (well 2/1-6) which are presence of micro-quartz and clay coatings. And the reason for low porosity zones in Tambar and Ula Fields is possibly the same as in Gyda Field which is that angular grains loose porosity when they are subjected to stress as compared to rounded grain sandstones. To confirm these findings author would suggest looking in to the samples from Tambar and Ula Fields.

7.6. IGV

IGV (Inter granular volume) is the sum of intergranular porosity, cement, and the matrix (Paxton et al. 2002). Average IGV in the study is 31.5% and ranges from 14% to 44% (Figure 6.4). Reason for high IGV in the study is high matrix content. Several factors can affect the IGV of the sandstone which will be discussed separately here.

7.6.1. CARBONATE CEMENT

In most of the samples studied, carbonate cement was observed (Table 6.1, Appendix E). This carbonate cement (mostly dolomite) occurs by filling the pore space which might have cemented the sandstone at early stages of mechanical compaction later resulting in high IGV.

7.6.2. MECHANICAL COMPACTION

Grains of sandstones have been deformed in different styles and were observed in thin section study (Figure 6.18 a-1). This deformation involves the fracturing of grains, grain crushing, and compaction of grains. Grain crushing and deformed grains were observed in the study of thin sections under optical microscope. Grain deformation is done by sliding and reorientation of the grains. This observation is in agreement with Bjørlykke (1998, 1999, 2003) who proposed that the mechanical compaction involves rearrangement of grains, ductile bending of grains and breakage of grains. Though ductile deformation was not observed in the study. All of these processes are most likely to reduce the porosity and in turn IGV of the sandstones.

Figure 6.4 show that we have a very nice correlation between IGV and matrix. With increasing matrix, IGV also increases. We have high percentage of IGV in samples from Ula A and Ula C as these zones have high amount of matrix content (Appendix B). Here matrix is defined as depositional clay and silt size particles which fill the space between framework grains. As sandstones are subjected to mechanical compaction grain frame is locked. Porosity starts to decrease because of grain crushing, reorientation and deformation. Sandstones which have clay/matrix in between them show little subsequent grain reorientation. This is probably due to soft grain contacts due to matrix in between grains. Chuhan et al (2002, 2003) proved that coarse grained sandstones are compacted more as compared to fine grained sandstones. This study is in analogy with Chuhan et al (2002, 2003) as Ula A and C which are fine grained sandstones (Appendix B) have high IGV as compared to Ula B which is coarse grained sandstone.

All the samples of the sandstones of Ula Formation from well 2/1-6 are medium to fine grained and are both poorly and well sorted. Seven samples from Ula B, which is the most important high porosity zone of the well 2/1-6, are medium to fine grained and are mostly moderately sorted. Samples from Ula A and Ula C are well sorted and fine grained (Appendix B). Though coarse grained samples were not observed so medium and fine grained sandstones were compared. Experimental compaction done by Chuhan et al (2002, 2003) proved that well sorted coarse grain sandstones compact more and loose porosity as compared to the fine grained and poorly sorted sandstones. This is the reason that samples from Ula B (medium grain size) show less porosity on thin sections. While samples from Ula A and C (fine grain size) show high porosity (Appendix C). So this study is in consistent with findings of Chuhan et al (2002, 2003).

7.6.3. GRAIN SIZE

Average grain size in the studied samples ranges from medium to fine grain. Samples from Ula B are medium grain size and samples from Ula A and C are fine grained. As no coarse grain sandstone was observed in study, so medium and fine grained samples were compared. Average IGV of medium grained samples is 26% while fine grained samples have 34% IGV (Appendix B) which implies that medium grained sandstones have less IGV as compared to fine grained sandstones. Coarse/medium grained sandstones are more crushed and compacted as compared to

fine grained sandstones which imply that coarse grained sandstones would have less IGV as compared to fine grained sandstones.

7.6.4. GRAIN SORTING

Samples from Ula A and C are mostly well sorted. Samples from Ula B are poorly and moderately sorted. Studies like done by Rogers and Head (1961), Beard and Weyl (1973) have proved that well sorted sandstones have higher IGV as compared to moderately and poorly sorted. These findings are in agreement with the study (Appendix B). Samples from Ula A and C have high IGV while samples from Ula B have low IGV.

7.6.5. GRAIN SHAPE

Most common shape of grain in the study was the angular grains (11 samples). Sub-rounded grains were present as second majority (7 samples) but there were only two samples of with sub-angular grains. Average IGV of angular grains calculated through point counting is 34%. Average IGV of sub-rounded grins is 28%. While sub-angular samples have average IGV of 30%. This clearly indicates that samples with angular grains have high IGV while sub-rounded grains have less IGV as compared to sub-angular and angular grains.

8. CONCLUSION

CONCLUSION

- Micro-quartz grain coating is very common in the study area. Clay grain coatings are also present and Illite is the most common clay grain coating as compared to chlorite grain coating. Micro-quartz grain coating seems to be the main cause of preserving porosity at depths of > 4000m in the Ula B zone.
- Micro-quartz is present in all samples in both high and low porosity zones. It is most likely that it is present in all zones because of sedimentary reworking of the sponge spicule Rhaxella Perforata.
- Grain shape has pronounced effect on porosity of the sandstones in the area. Angular grains loose porosity with mechanical compaction as they have small contact areas and this promotes deformation resulting in porosity loss. Perhaps this is the reason that Ula A and Ula C have low porosities.
- Inter Granular Volume is very high in the study area (up to 44%). Reason for high IGV in most of the samples is high amount of matrix. IGV depends on many factors including mechanical compaction, grain sorting, grain size, and grain shape.
- IGV is higher in fine grained sandstones as compared to medium grained sandstones.

9. REFERENCES

AAGAARD, P., EGEBERG, P. K., SAIGAL, G. C., MORAD, S. & BJORLYKKE, K. 1990. Diagenetic albitization of detrital K-feldspars in Jurassic, Lower Cretaceous and Tertiary clastic reservoir rocks from offshore Norway; II, Formation water chemistry and kinetic considerations. *Journal of Sedimentary Research,* 60**,** 575-581.

AASE, N. E., & O. WALDERHAUG 2005. The effect of hydrocarbons on quartz cementation: Diagenesis in the Upper Jurassic sandstones of the Miller field, North Sea, revisited. *Petroleum Geoscience,* 11**,** 215–223.

AASE, N. E., BJORKUM, P. A. & NADEAU, P. H. 1996. The effect of grain-coating microquartz on preservation of reservoir porosity. *AAPG Bulletin,* 80**,** 1654-1673.

AJDUKIEWICZ, J. M. & LANDER, R. H. 2010. Sandstone reservoir quality prediction: The state of the art. *AAPG Bulletin,* 94**,** 1083-1091.

ANDREWS, I. J. & BROWN, S. 1987. Stratigraphic evolution of the Jurassic, Moray Firth,. *In:* BROOKS, J. & K. W. GLENNIE (eds.) *Petroleum Geology of North West Europe.* London: Graham & Trotman.

ANJOS, S. M. C., DE ROS, L. F. & SILVA, C. M. A. 2009. Chlorite Authigenesis and Porosity Preservation in the Upper Cretaceous Marine Sandstones of the Santos Basin, Offshore Eastern Brazil. *Clay Mineral Cements in Sandstones.* Blackwell Publishing Ltd.

BARCLAY, S. A. & WORDEN, R. H. 2000b. *Petrophysical and Petrographical Analysis of Quartz Cement Volumes across Oil–Water Contacts in the Magnus Field, Northern North Sea*, Blackwell Publishing Ltd.

BEACH, A. 1986. Some comments on sedimentary basin development in the Northern North Sea. *Scottish Journal of Geology,* 21**,** 493-512.

BEARD, D. C. & WEYL, P. K. 1973. Influence of Texture on Porosity and Permeability of Unconsolidated Sand. *AAPG Bulletin,* 57**,** 349-369.

BJORKUM, P. A. 1996. How important is pressure in causing dissolution of quartz in sandstones? *Journal of Sedimentary Research,* 66**,** 147-154.

BJØRLYKKE, K. 1998. Clay mineral diagenesis in sedimentary basins; a key to the prediction of rock properties; examples from the North Sea Basin. *Clay Minerals,* 33**,** 15-34.

BJØRLYKKE, K. 1994. Pore water flow and mass transfer of solids in solution in sedimentary basins. . *In:* PARKER, A. & SELLWOOD, B. W. (eds.) *Quantitative Diagenesis: Recent Developments and Applications to Reservoir Geology.*: Kluwer Dordrecht.

BJØRLYKKE, K. 1999. An overview of factors controlling rates of compaction and fluid flow in sedimentary basins. *In:* JAMTVEIT, B. & MEAKIN, P. (eds.) *Growth, dissolution and pattern formation in geosystems.* Netherlands: Kluwer Academic Publishers.

BJØRLYKKE, K. 2003. Compaction (consolidation) of sediments. *In:* MIDDLETON, G. V. (ed.) *Encyclopedia of Sediments and Sedimentary Rocks.* Kluwer Academic Publishers.

BJØRLYKKE, K. 2010. From Sedimentary Environments to Rock Physics. *Petroleum Geoscience***,** 114-130.

BJØRLYKKE, K. & AAGAARD, P. 1992. CLAY MINERALS IN NORTH SEA SANDSTONES. *Origin, Diagenesis, and Petrophysics of Clay Minerals in Sandstones.* SEPM (Society for Sedimentary Geology).

BJØRLYKKE, K., NEDKVITNE, T., RAMM, M. & SAIGAL, G. C. 1992. Diagenetic processes in the Brent Group (Middle Jurassic) reservoirs of the North Sea: an overview. *Geological Society, London, Special Publications,* 61**,** 263-287.

BJØRLYKKE, K., RAMM, M. & SAIGAL, G. 1989. Sandstone diagenesis and porosity modification during basin evolution. *Geologische Rundschau,* 78**,** 243-268.

BLOCH, S., LANDER, R. H. & BONNELL, L. 2002. Anomalously High Porosity and Permeability in Deeply Buried Sandstone Reservoirs: Origin and Predictability. *AAPG Bulletin,* 86**,** 301-328.

BROOKS, J. & GLENNIE, K. W. 1987. Petroleum Geology of North West Europe. 1209.

CANNON, S. J. C. & GOWLAND, S. 1996. Facies controls on reservoir quality in the Late Jurassic Fulmar Formation, Quadrant 21, UKCS. *Geological Society, London, Special Publications,* 114**,** 215-233.

CHOH, S.-J., MILLIKEN, K. L. & MCBRIDE, E. F. 2003. A tutorial for sandstone petrology: architecture and development of an interactive program for teaching highly visual material. *Computers & Geosciences,* 29**,** 1127-1135.

CHUHAN, F. A., BJØRLYKKE, K. & LOWREY, C. 2000. The role of provenance in illitization of deeply buried reservoir sandstones from Haltenbanken and north Viking Graben, offshore Norway. *Marine and Petroleum Geology,* 17**,** 673-689.

CHUHAN, F. A., KJELDSTAD, A., BJØRLYKKE, K. & HØEG, K. 2002. Porosity loss in sand by grain crushing--experimental evidence and relevance to reservoir quality. *Marine and Petroleum Geology,* 19**,** 39-53.

CHUHAN, F. A., KJELDSTAD, A., BJØRLYKKE, K. & HØEG, K. 2003. Experimental compression of loose sands: relevance to porosity reduction during burial in sedimentary basins. *Canadian Geotechnical Journal,* 40**,** 995-1011.

CORNFORD, C. 2009. Source Rocks and Hydrocarbons of the North Sea. *Petroleum Geology of the North Sea.* Blackwell Science Ltd.

DEEGAN, C. E. & SCULL, J. 1977. *A proposed standard lithostratigraphic nomenclature for the central and Northern North-Sea*.

EHRENBERG, S. N. 1993. Preservation of anomalously high porosity in deeply buried sandstones by grain-coating chlorite; examples from the Norwegian continental shelf. *AAPG Bulletin,* 77**,** 1260-1286.

EMERY, D., SMALLEY, P. C., OXTOBY, N. H., RAGNARSDOTTIR, K. V., AAGAARD, P., HALLIDAY, A., COLEMAN, M. L. & PETROVICH, R. 1993. Synchronous Oil Migration and Cementation in Sandstone Reservoirs Demonstrated by Quantitative Description of Diagenesis [and Discussion]. *Philosophical Transactions: Physical Sciences and Engineering,* 344**,** 115-125.

ERRATT, D., THOMAS, G. M. & WALL, G., R, T. 1999. The evolution of the Central North Sea Rift: Petroleum Geology of Northwest Europe. *Proceedings of the 5th Conference, Geological Society of London***,** 63-82.

EVANS, D., GRAHAM, C., ARMOUR, A. & BATHURST, P. 2003. Millennium atlas; Petroleum geology of the central and northern North Sea. *Geological Magazine,* 140**,** 487-.

FASSI-FIHRI, O., ROBIN, M. & ROSENBERG, E. 1991. Wettability studies at the pore level: a new approach by the use of cryo-scanning electron microscopy. *SPE Formation Evaluation,* Volume 10, Number 1**,** 11-19.

FAWAD, M., MONDOL, N. H., JAHREN, J. & BJØRLYKKE, K. 2011. Mechanical compaction and ultrasonic velocity of sands with different texture and mineralogical composition. *Geophysical Prospecting***,** no-no.

FISHER, Q., KNIPE, R. & WORDEN, R. H. 2000. *The relationship between faulting, fractures, transport of silica and quartz cementation in North Sea oil fields*, Blackwell Science, Oxford.

FRASER, S. I., ROBINSON, A. M., JOHNSON, H. D., UNDERHILL, J. R., KADOLSKY, D. G. A., CONNELL, R., JOHANNESSEN, P. & RAVNÅS, R. 2002. Upper Jurassic. *In:* EVANS, D., ARMOUR, A. & BATHURST, P. (eds.) *Millennium Atlas: petroleum geology of the central and northern North Sea.* London: The Geological Society of London.

GABRIELSEN, R. H. 1986. Structural elements in graben systems and their influence on hydrocarbon trap types. *In:* M, S. A. (ed.) *Habitat of Hydrocarbons on the Norwegian Continental Shelf.* London: Graham and Trotman, Norwegian Petroleum Soceity.

GIBBS, A. D. 1989. Structural Styles in basin formation. *In:* TANKARD, A. J. & BALKWILL, H. R. (eds.) *Extensional Tectonics of the north Atlantic margins*
AAPG Memoir.
GILES, M. R., STEVENSON, S., MARTIN, S. V., CANNON, S. J. C., HAMILTON, P. J., MARSHALL, J. D. & SAMWAYS, G. M. 1992. The reservoir properties and diagenesis of the Brent Group: a regional perspective. *Geological Society, London, Special Publications,* 61**,** 289-327.
GLENNIE, K. W. 1998. *Petroleum Geology of the North Sea. Basic concepts and recent advances*, Blackwell Science.
GLUYAS, J. G., GRANT, S. M. & ROBINSON, A. 1993. Geochemical evidence for a temporal link control on sandstone cementation. *Diagenesis and Basin Development.* Association of Petroleum Geologists Studies in Geology
GOWERS, M., HOLTAR, E. & SWENSSON, E. 1993. The structure of the Norwegian Central trough (Central Graben area). *Petroleum Geology of Northwest Europe: Proceedings of the 4th Conference.*
GOWLAND, S. 1996. Facies characteristics and depositional models of highly bioturbated shallow marine siliciclastic strata: an example from the Fulmar Formation (Late Jurassic), UK Central Graben. *In:* HURST., A., JOHNSON., H. D., BURLEY., S. D., CANHAM., A. C. & MACKERTICH., D. S. (eds.). Geological Society of London.
GÖTZE, J., PLÖTZE, M. & HABERMANN, D. 2001. Origin, spectral characteristics and practical applications of the cathodoluminescence (CL) of quartz – a review. *Mineralogy and Petrology,* 71**,** 225-250.
HEALD, M. T. & E., Larese. R. 1974. Influence of coatings on quartz cementation. *Journal of Sedimentary Petrology,* 44**,** 1269-1274.
HENDRY, J. P. & TREWIN, N. H. 1995. Authigenic quartz microfabrics in Cretaceous turbidites; evidence for silica transformation processes in sandstones. *Journal of Sedimentary Research,* 65**,** 380-392.
HENDRY, J. P. & TREWIN., N. H. 1995. Authigenic quartz microfabrics in Cretaceous turbidites: evidence for silica transformation processes in sandstones. *Journal of Sedimentary research,* A65**,** 380-392.
HINDE, G. J. 1890. On a new Genus of Siliceous Sponges from the Lower Calcareous Grit of Yorkshire. *Quarterly Journal of the Geological Society,* 46**,** 54-60,NP,61.
JAHREN, J. & RAMM, M. 2000. *The Porosity-Preserving Effects of Microcrystalline Quartz Coatings in Arenitic Sandstones: Examples from the Norwegian Continental Shelf*, Blackwell Publishing Ltd.
JOHNSON, R. H. 1920. The cementation process in sandstones. *AAPG Bulletin,* 4**,** 33-35.
LANDER, R. H., LARESE, R. E. & BONNELL, L. M. 2008. Toward more accurate quartz cement models: The importance of euhedral versus noneuhedral growth rates. *AAPG Bulletin,* 92**,** 1537-1563.
LONGIARU, S. 1987. Visual comparators for estimating the degree of sorting from plane and thin section. *Journal of Sedimentary Research* 57**,** 791.
MALIVA, R. G. & SIEVER, R. 1988. Pre-Cenozoic nodular cherts: Evidence for opal-CT precursors and direct quartz replacement. *American Journal of Science,* 288**,** 798-809.
MARTIN, M. A. & POLLARD, J. E. 1996. The role of trace fossil (ichnofabric) analysis in the development of depositional models for the Upper Jurassic Fulmar Formation of the Kittiwake Field (Quadrant 21 UKCS). *Geological Society, London, Special Publications,* 114**,** 163-183.
MAST, T. E. 2008. *Reservoir quality of deeply buried, Upper Jurassic sandstones of the South Viking Graben.* Masters in PEGG, University of Oslo.
MCBRIDE, E. F. 1989. Quartz cement in sandstones: a review. *Earth-Science Reviews,* 26**,** 69-112.
MCKENZIE, D. 1978. Some remarks on the development of sedimentary basins. *Earth and Planetary Science Letters,* 40**,** 25-32.
MORAD, S., BEN ISMAIL, H. N., DE ROS, L. F., AL-AASM, I. S. & SERRHINI, N. E. 1994. *Diagenesis and Formation Water Chemistry of Triassic Reservoir Sandstones from Southern Tunisia*, Blackwell Publishing Ltd.

NOTTVEDT, A., GABRIELSEN, R. H. & STEEL, R. J. 1995. Tectonostratigraphy and sedimentary architecture of rift basins, with reference to the northern North Sea. *Marine and Petroleum Geology,* 12**,** 881-901.

OELKERS, E. H., BJØRKUM, P. A., WALDERHAUG, O., NADEAU, P. H. & MURPHY, W. M. 2000. Making diagenesis obey thermodynamics and kinetics: the case of quartz cementation in sandstones from offshore mid-Norway. *Applied Geochemistry,* 15**,** 295-309.

PAXTON, S. T., SZABO, J. O., AJDUKIEWICZ, J. M. & KLIMENTIDIS, R. E. 2002. Construction of an Intergranular Volume Compaction Curve for Evaluating and Predicting Compaction and Porosity Loss in Rigid-Grain Sandstone Reservoirs. *AAPG Bulletin,* 86**,** 2047-2067.

PEMBERTON, S. G., MACEACHERN, J. A. & FREY, R. W. 1992. Trace fossil models: environmental and allostratigraphic significance. *In:* WALKER, R. G. & JAMES, N. P. (eds.) *Facies Models - Response to Sea-Level Change.*: St. John's, NFD: Geological Association of Canada.

PETTIJOHN, J., POTTER., P. E. & SIEVER., R. 1987. *Sand and Sandstone,* New York, Springer Verlag.

PITTMAN, E. D., LARESE, R. E. & HEALD, M. T. 1992. Clay coats: occurrence and relevance to preservation of porosity in sandstones. *In:* HOUSEKNECHT, D. W. & PITTMAN, E. D. (eds.) *Origin, diagenesis, and petrophysics of clay minerals in sandstones.*

RAMM, M. & BJORLYKKE, K. 1994. Porosity/depth trends in reservoir sandstones; assessing the quantitative effects of varying pore-pressure, temperature history and mineralogy, Norwegian Shelf data. *Clay Minerals,* 29**,** 475-490.

RAMM, M. & FORSBERG., A. W. 1991. *Porosity versus depth trends in Upper Jurassic sansdtones from the Cod - Terrace area, central North Sea.* University of Oslo.

RAMM, M., FORSBERG., A. W. & JAHREN., J. J. 1997. Porosity depth trends in deeply buried Upper Jurassic reservoirs in Norwegian Central Graben: An example of porosity preservation beneath the normal economic basement by grain coating microquartz. *AAPG Memoir 69***,** 177-199.

RAVNÅS, R., NØTTVEDT, A., STEEL, R. J. & WINDELSTAD, J. 2000. Syn-rift sedimentary architectures in the Northern North Sea. *Geological Society, London, Special Publications,* 167**,** 133-177.

ROBERTS, A. M., PRICE, J. D. & OLSEN, T. S. 1990. Late Jurassic half-graben control on the siting and structure of hydrocarbon accumulations: UK/Norwegian Central Graben. *Geological Society, London, Special Publications,* 55**,** 229-257.

ROBERTS, A. M. & YIELDING, G. 1991. Deformation around basin-margin faults in the North Sea/mid-Norway rift. *Geological Society, London, Special Publications,* 56**,** 61-78.

ROGERS, J. J. W. & HEAD, W. B. 1961. Relationships between porosity, median size, and sorting coefficients of synthetic sands. *Journal of Sedimentary Research,* 31**,** 467-470.

RUTTER, E. H. & ELLIOTT, D. 1976. The Kinetics of Rock Deformation by Pressure Solution [and Discussion]. *Philosophical Transactions of the Royal Society of London. Series A, Mathematical and Physical Sciences,* 283**,** 203-219.

RØNNEVIK, H., VAN DEN BOSCH, W. & BANDLIEN, E. 1975. A proposed nomenclature for the main structural features in the Norwegian North Sea. 28-30.

SAIGAL, G. C. & BJØRLYKKE, K. 1987. Carbonate cement in clastic reservoir rocks from offshore Norway - relationship between isotopic composition, textural development and burial depth. *In:* D., M. M. (ed.) *The diagenesis of Sedimentary Sequences.* Geol. Soc. London.

SAIGAL, G. C., MORAD, S., BJORLYKKE, K., EGEBERG, P. K. & AAGAARD, P. 1988. Diagenetic albitization of detrital K-feldspar in Jurassic, Lower Cretaceous, and Tertiary clastic reservoir rocks from offshore Norway; I, Textures and origin. *Journal of Sedimentary Research,* 58**,** 1003-1013.

SEARS, R. A., HARBURY, A. R., PROTOY, A. J. G. & STEWART, D. J. 1993. Structural styles from the Central Graben in the UK and Norway. *Geological Society, London, Petroleum Geology Conference series,* 4**,** 1231-1243.

SINCOCK, K. J. & BLACK, C. J. J. 1988. Validation of water/oil displacement scaling criteria using microvisualisation techniques. *Proceedings of the 64th Annual Technical Conference and Exhibition of the Society of Petroleum Engineers* SPE 18294**,** 339-347.

SKJERVEN, J., RIJS, F. & KALHEIM, J. 1983. Late Paleozoic to Early Cenozoic structural development of the south-southeastern Norwegian North Sea. Geologie en Mijnbouw 62**,** 35-45.

SMITH, R. I., HODGSON, N. & FULTON, M. 1993. Salt control on Triassic reservoir distribution, UKCS Central North Sea. *Geological Society, London, Petroleum Geology Conference series,* 4**,** 547-557.

SPARK, I. S. C. & TREWIN., N. H. 1986. Facies related diagenesis in the main Claymore oilfield sandstones. *Clay Minerals,* 21**,** 479-496.

TALBOT, M. R. 1973. Major sedimentary cycles in the Corallian Beds (Oxfordian) of southern England: Palaeogeography, Palaeoclimatology, Palaeoecology. 14**,** 293-317.

TAYLOR, A. M. & GAWTHORPE, R. L. 1993. Application of sequence stratigraphy and trace fossil analysis to reservoir description: examples from the Jurassic of the North Sea. *Geological Society, London, Petroleum Geology Conference series,* 4**,** 317-335.

TAYLOR, T., STANCLIFFE, R., MACAULAY, C. & HATHON, L. 2004. High temperature quartz cementation and the timing of hydrocarbon accumulation in the Jurassic Norphlet sandstone, offshore Gulf of Mexico, USA. *Geological Society, London, Special Publications,* 237**,** 257-278.

TAYLOR, T. R., GILES, M. R., HATHON, L. A., DIGGS, T. N., BRAUNSDORF, N. R., BIRBIGLIA, G. V., KITTRIDGE, M. G., MACAULAY, C. I. & ESPEJO, I. S. 2010. Sandstone diagenesis and reservoir quality prediction: Models, myths, and reality. *AAPG Bulletin,* 94**,** 1093-1132.

THOMSON, A. 1979. Preservation of porosity in the deep Woodbine/Tuscaloosa trend, Louisiana. *Gulf Coast Association of Geological Societies Transactions,* 30**,** 396–403.

VAGLE, G. B., HURST, A. & DYPVIK, H. 1994. Origin of quartz cements in some sandstones from the Jurassic of the Inner Moray Firth (UK). *Sedimentology,* 41**,** 363-377.

VAN DER HELM, A. A., GRAY., D. I., COOK., M. A. & SCHULTE., A. M. 1990. Fulmar: The development of a large North Sea Field. *In:* BULLER., A. T., BERG., E., HJELMELAND., O., KLEPPE., J., TORSÆTER., O. & AASEN., J. O. (eds.) *North Sea Oil & Gas reservoirs -II.* Graham & Trotman.

VOLLSET, J. & DORÊ, A. G. 1984. A revised triassic and Jurassic lithostratigraphic nomenclature for the Norwegian North-Sea. *Bull. NPD,* 3.

WALDERHAUG, O. 1994a. Precipitation rates for quartz cement in sandstones determined by fluid-inclusion microthermometry and temperature-history modeling. *Journal of Sedimentary Research,* 64**,** 324-333.

WALDERHAUG, O. 1996. Kinetic modeling of quartz cementation and porosity loss in deeply buried sandstone reservoirs. *AAPG Bulletin,* 80**,** 731-745.

WILSON, R. C. L. 1968. Carbonate facies variation within the Osmington oolite series in southern England: Palaeogeography, Palaeoclimatology, Palaeoecology. 4**,** 89-123.

WORDEN, R. H. & MORAD, S. 2000. Quartz Cementation in oil field sandstones: a review of the key controversies. *In:* WORDEN, R. H. & MORAD, S. (eds.) *Quartz Cementation in Sandstones.* Blackell Science.

WWW.NPD.NO

ZANELLA, E. & COWARD, M. P. 2003. Structural framework. *In:* EVANS, D., GRAHAM, C., ARMOUR, A. & BATHURST, P. (eds.) *Millennium Atlas.* London: The Geological Society of London.

10. APPENDIX

APPENDIX A: WELL CORRELATION FROM RAMM ET AL, 1997

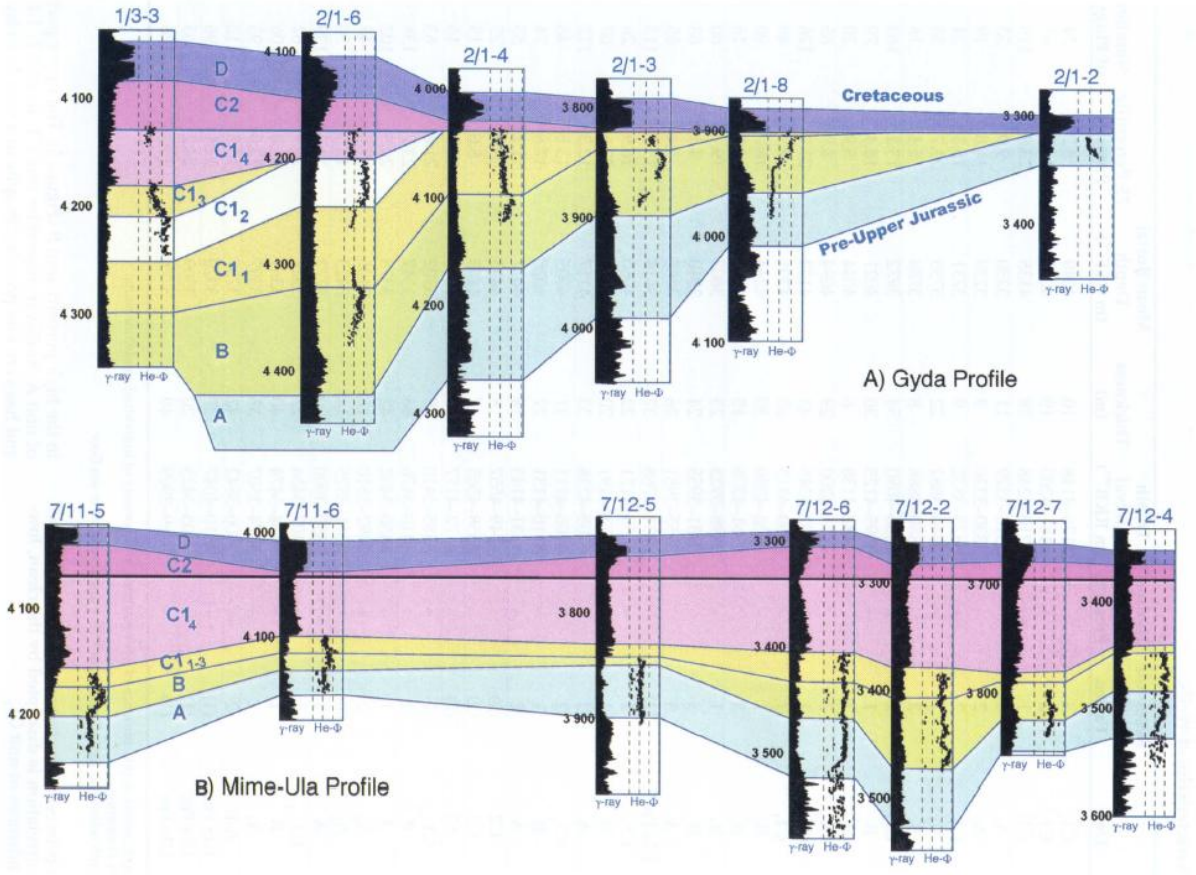

APPENDIX B: IGV AND GRAIN TEXTURAL DATA

Sample	Average Grain Size mm	IGV %	Sorting	Grain size	Grain Shape
2-12	0.25	37.2	Well sorted	Medium grained	Angular
2-14	0.0175	32.2	Moderately sorted	Fine grained	Angular
2-15	0.0175	33.9	Well sorted	Fine grained	Sub-angular
2-16	0.015	39.2	Well sorted	Fine grained	Angular
2-17	0.015	38.2	Well sorted	Fine grained	Angular
2-18	0.0175	30.3	Well sorted	Fine grained	Angular
2-19	0.01	26.9	Moderately sorted	Fine grained	Angular
2-21	0.02	21.6	Poorly sorted	Fine grained	Angular
3	0.02	25.8	Moderately sorted	Fine grained	Sub-angular
4	0.25	13.6	Moderately sorted	Medium grained	Sub-rounded
5	0.255	25.8	Moderately sorted	Fine to medium grained	Sub-rounded
6	0.2525	23.5	Well sorted	Fine to medium grained	Sub-rounded
7	0.0175	18.2	Well sorted	Medium grained	Sub-rounded
9	0.25	37.2	Poorly sorted	Medium grained	Sub-rounded
10	0.0175	26.5	Poorly sorted	Fine grained	Angular
11	0.02	41.2	Well sorted	Fine grained	Sub-rounded
12	0.015	38.6	Well sorted	Fine grained	Angular
13	0.0125	40.5	Well sorted	Fine grained	Angular
14	0.0125	36.9	Well sorted	Fine grained	Sub-rounded
16	0.0125	44.2	Well sorted	Fine grained	Angular

APPENDIX C: POINT COUNTING DATA

LOG Porosity	Sample	Depth	Quartz	Feldspar	Rock Fragments	Matrix	Calcite cement	Quartz Cement	Authigenic Kaolinite	Illite	Spicules	Mica	Primary Porosity	Secondary Porosity	IGV	Clay Index
low	2-12	4205.8	48.6	6.6	0	15.6	4	1.3	2	3	0	2.3	16.3	0	37.2	6.661728395
low	2-14	4212.55	55.6	5.6	0	7.6	3.3	6.3	1.6	4	0	0.6	15	0	32.2	5.671942446
low	2-15	4218.5	54.3	9.6	0	10.6	3	4.3	1.3	1	0	0.3	15	1	33.9	9.618416206
low	2-16	4222.6	50.6	7	0	15.3	4.3	3	1.6	1.3	0.3	0.3	15.6	1	39.2	7.0256917
low	2-17	4227.35	51.3	6.3	0	18	2.6	2	2	1.6	0	0.3	15.6	0	38.2	6.331189084
low	2-18	4231.8	59.3	3.6	0	7	4	5	2.3	3.6	0	0.6	14.3	0	30.3	3.660708263
low	2-19	4233.7	62	5.6	0	8	3	1.6	2.3	1.3	0	1.6	14.3	0	26.9	5.620967742
low	2-21	4240.6	71.3	4.6	0	6	1.3	1	1	0.9	0	0.3	13.3	0	21.6	4.612622721
high	3	4252.5	63.3	8.3	0.3	6.3	5.3	4.6	0.6	0.3	0	0	9.6	0	25.8	8.304739336
high	4	4254.6	76.3	4	0.6	2.3	3	3.3	3.3	1.6	0	0.3	5	0	13.6	4.020969856
high	5	4303.65	64.6	6.3	0	9.6	1.6	5	3	0.6	0	0	8.6	1	25.8	6.309287926
high	6	4309.6	69.6	4.3	0	9.6	4.6	4	1	1.3	0	0	5.3	0	23.5	4.318678161
high	7	4318.67	74	3.6	0	8	3.3	2.6	0.6	3	0	0.3	4.3	0	18.2	3.640540541
high	9	4321.7	54.6	3	0	19	0.6	2.6	2.9	1	0.6	0.7	15	0	37.2	3.018315018
high	10	4324.9	56.6	5.3	0	11.3	1.6	4.3	0.6	9.3	0	1.3	9.3	0	26.5	5.464310954
low	11	4327.6	54	2.3	0.3	22.3	2.6	4	0.6	0.6	0	0.6	12.3	0	41.2	2.311111111
low	12	4333.1	54.3	2	0	17.3	6	4	2.6	2	0	0.3	11.3	0	38.6	2.036832413
low	13	4336.95	47.3	8	0	18.3	2.6	2	2.3	0.6	0	1	17.6	0	40.5	8.012684989
low	14	4344.3	54.6	1.6	0	14	6.3	1.3	4.6	2.3	0	0.3	14.3	1	36.9	1.642124542
low	16	4353	46	3.3	0.3	29.3	5.3	2.3	3.3	0	1	1.6	7.3	0	44.2	3.3

APPENDIX D: CROSS PLOTS

D.1. P-wave vs Density Porosity color coded with Gamma Ray

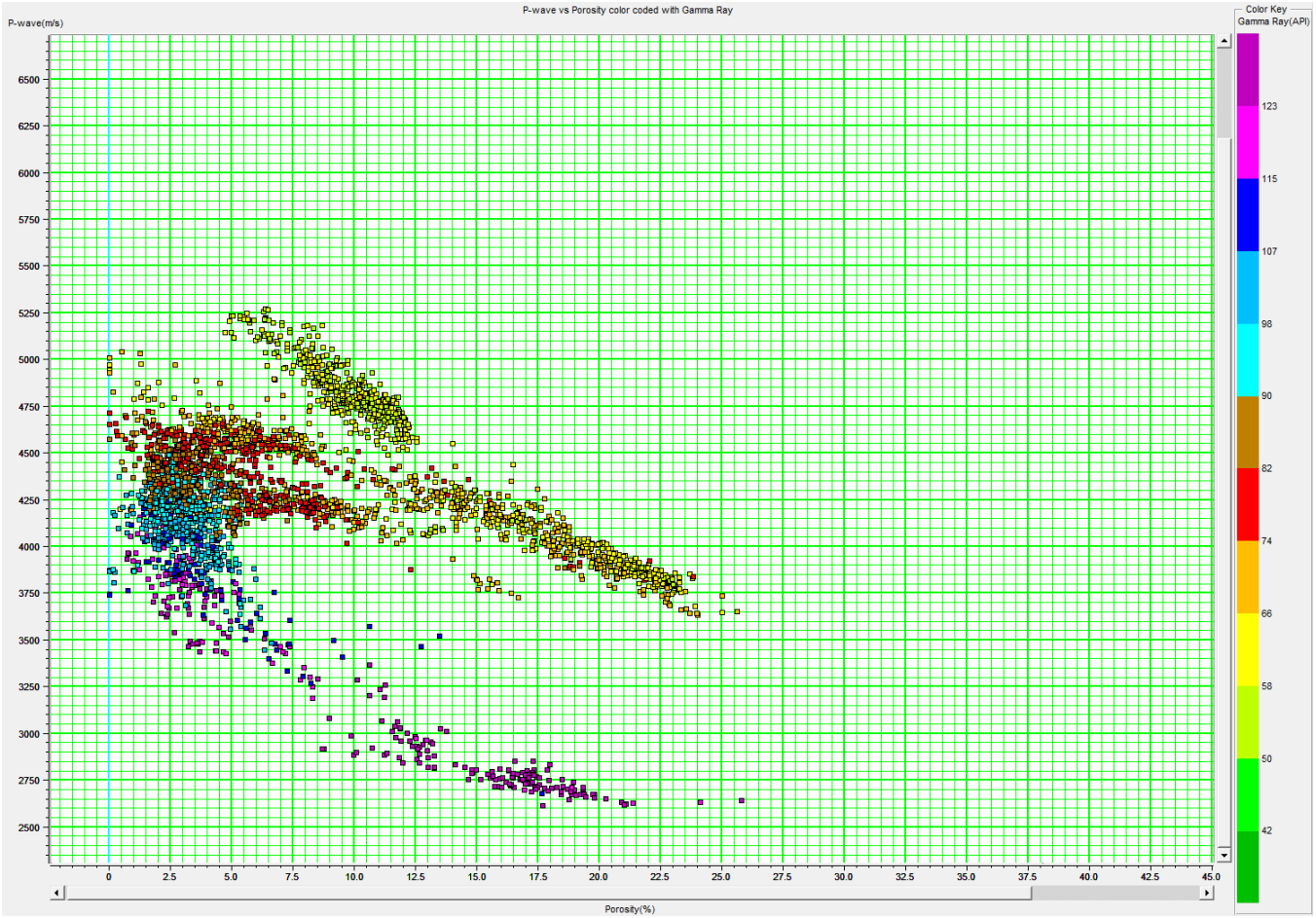

D.2. P-wave vs Density Porosity color coded with Vertical Depth

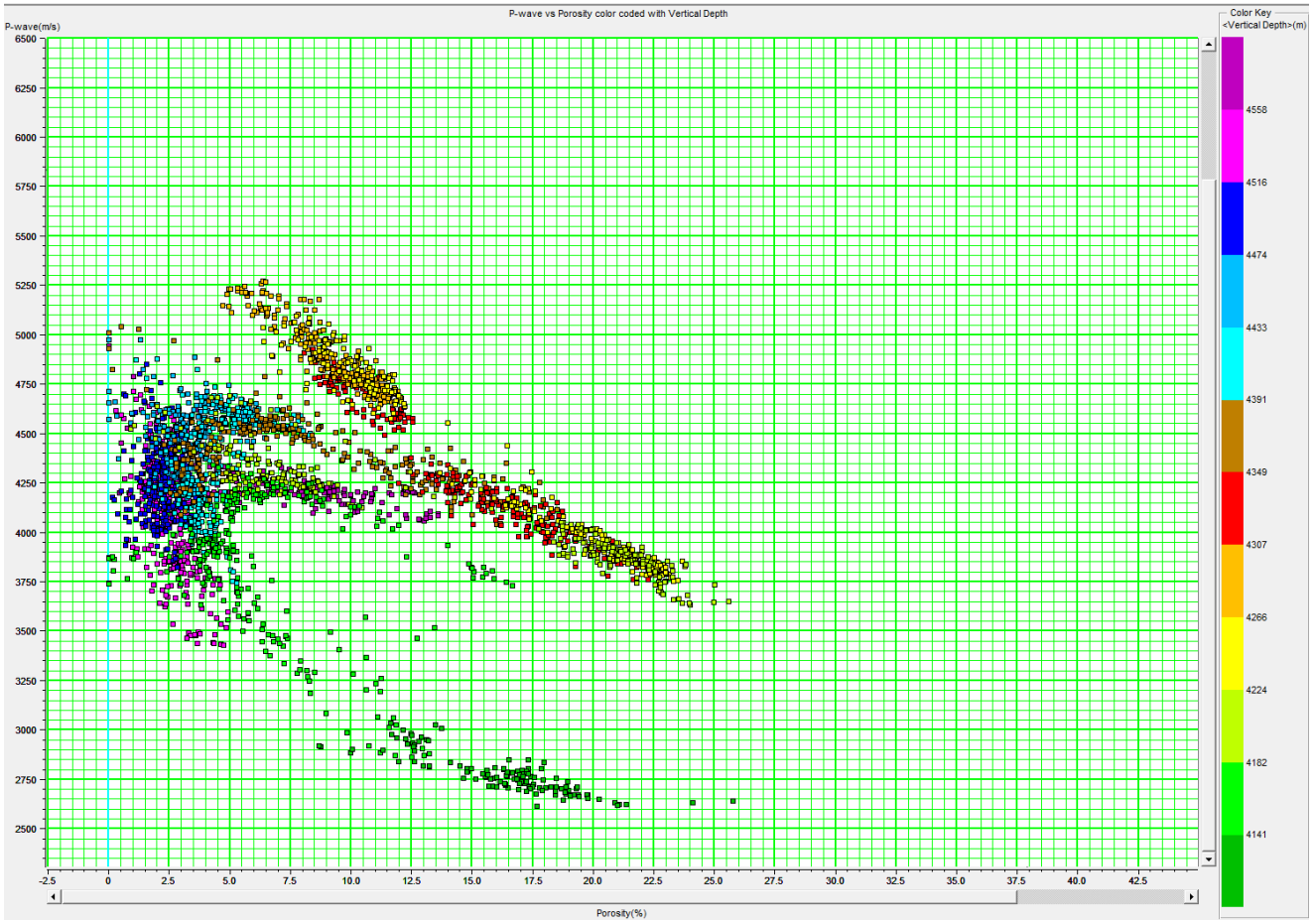

D.3. Neutron Porosity vs Density Porosity color coded with Vertical Depth

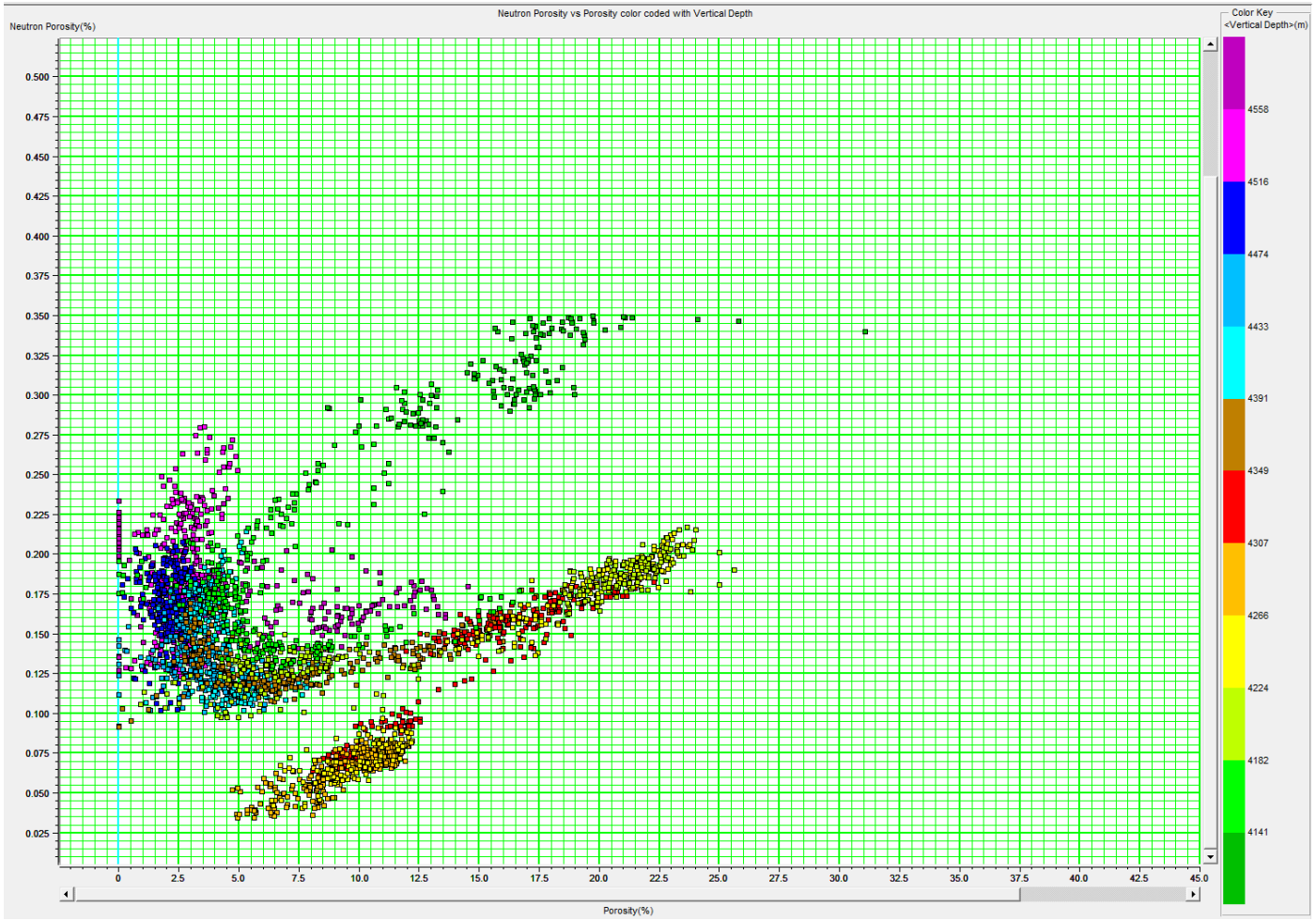

D.4. NEUTRON POROSITY VS DENSITY POROSITY COLOR CODED WITH GAMMA RAY

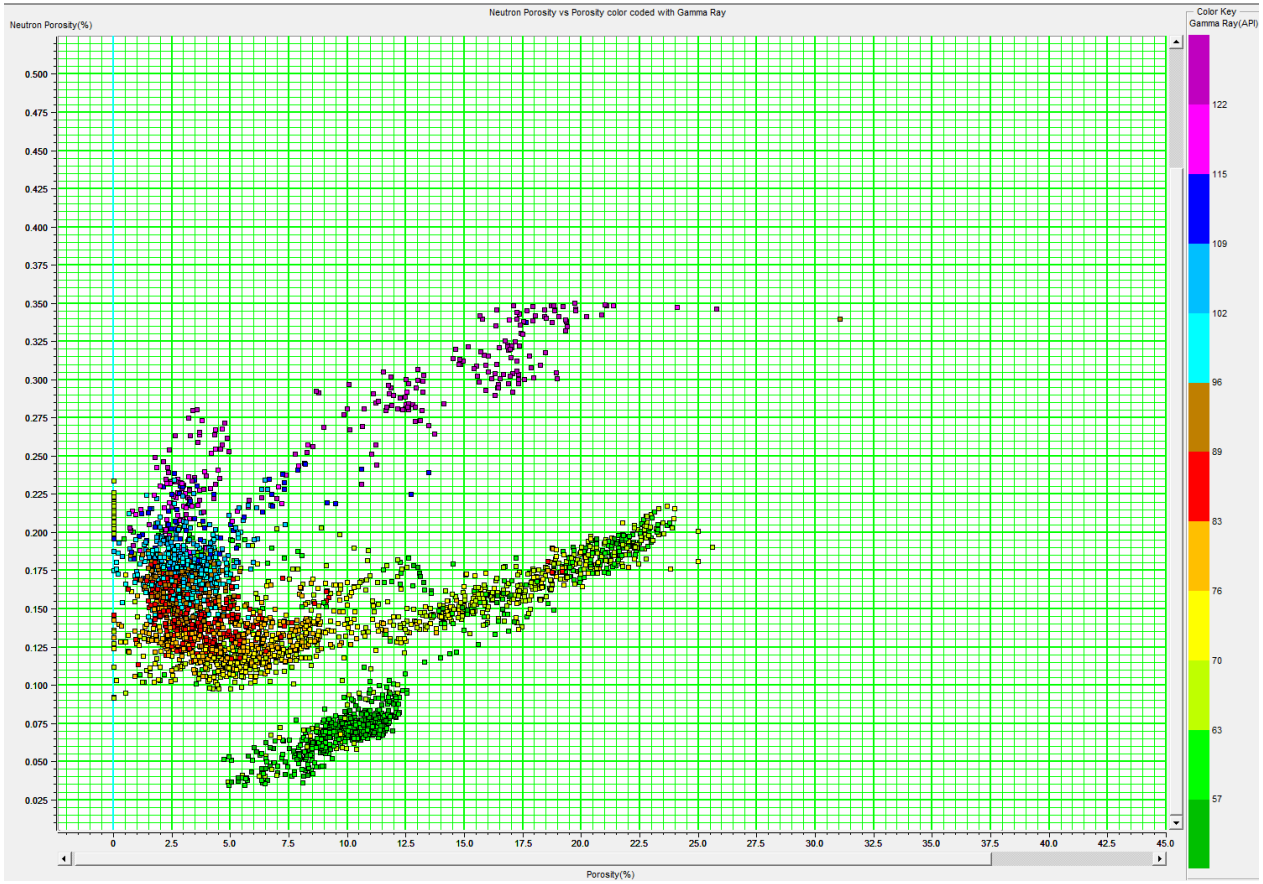

D.5. NEUTRON POROSITY VS DENSITY COLOR CODED WITH VERTICAL DEPTH

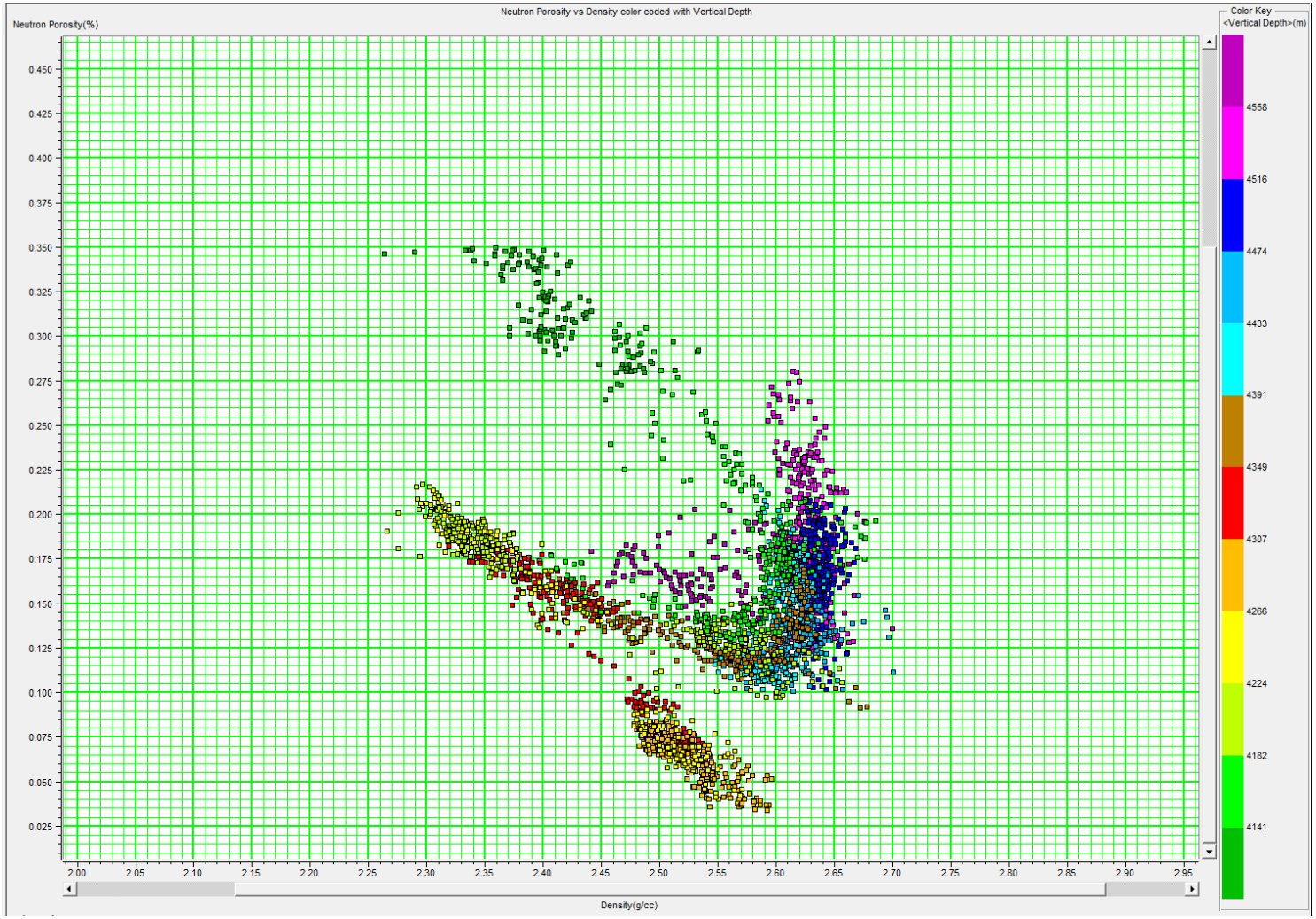

D.6. NEUTRON POROSITY VS DENSITY COLOR CODED WITH GAMMA RAY

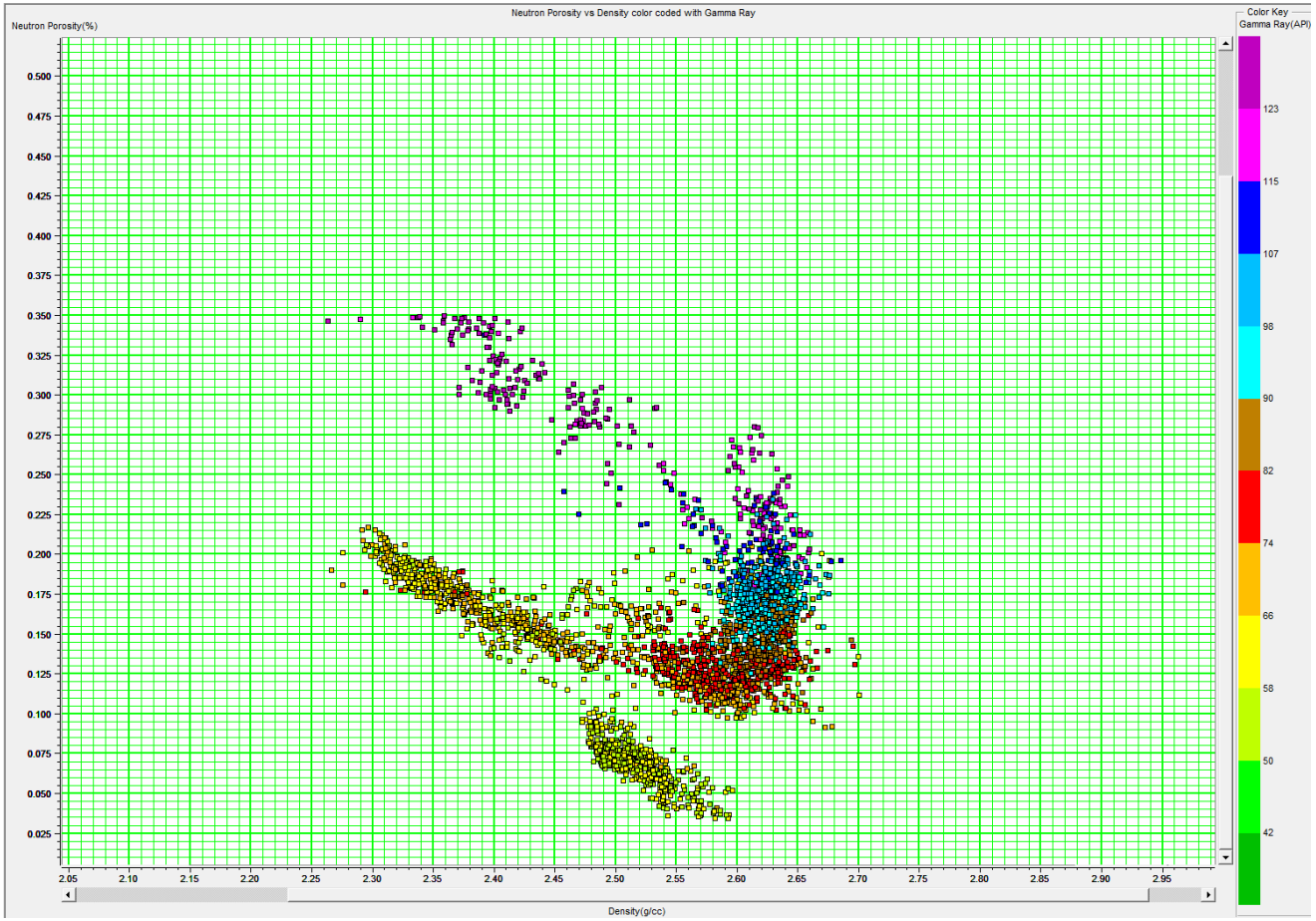

APPENDIX E: CARBONATE CEMENT IN SAMPLES

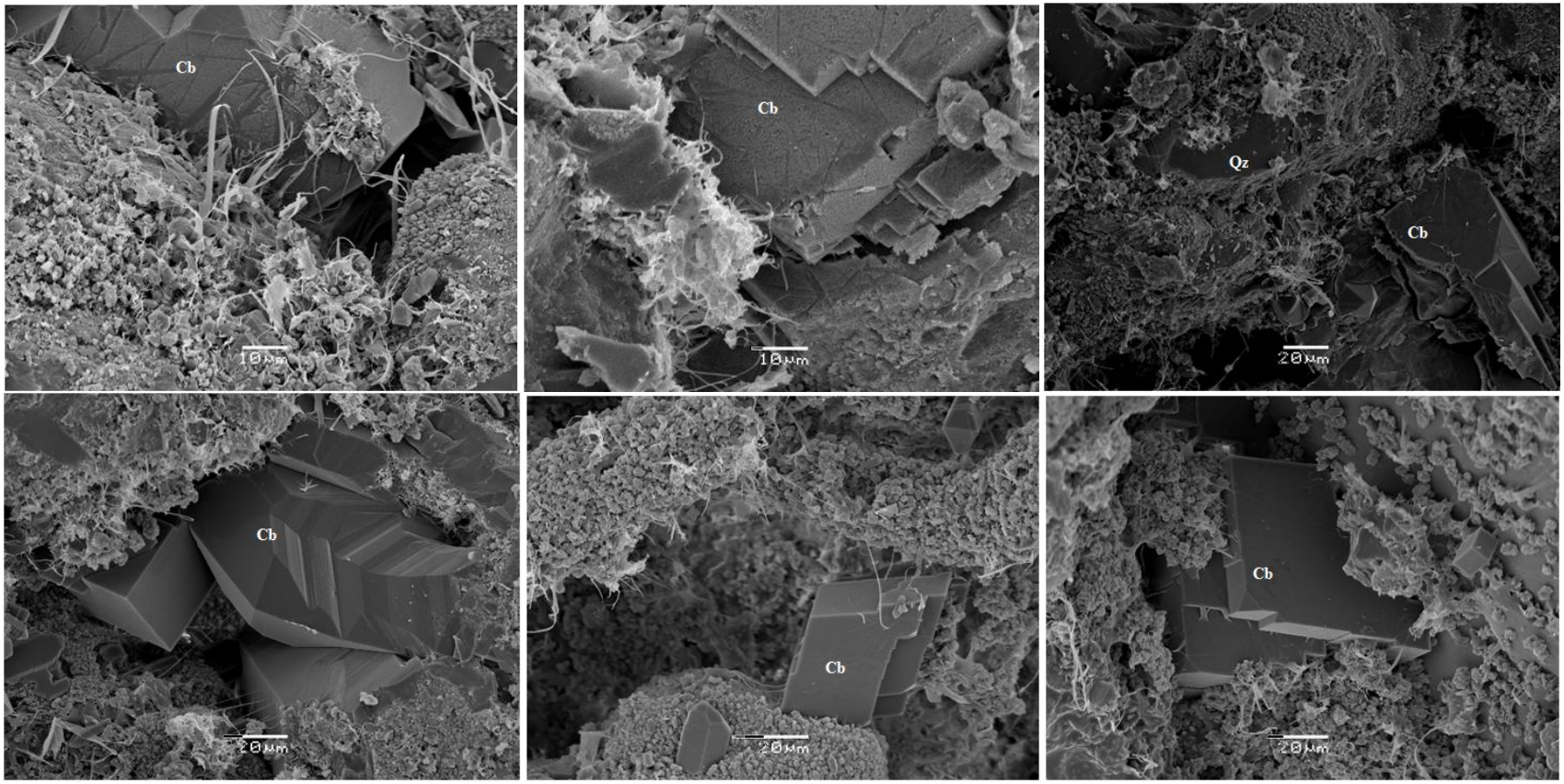

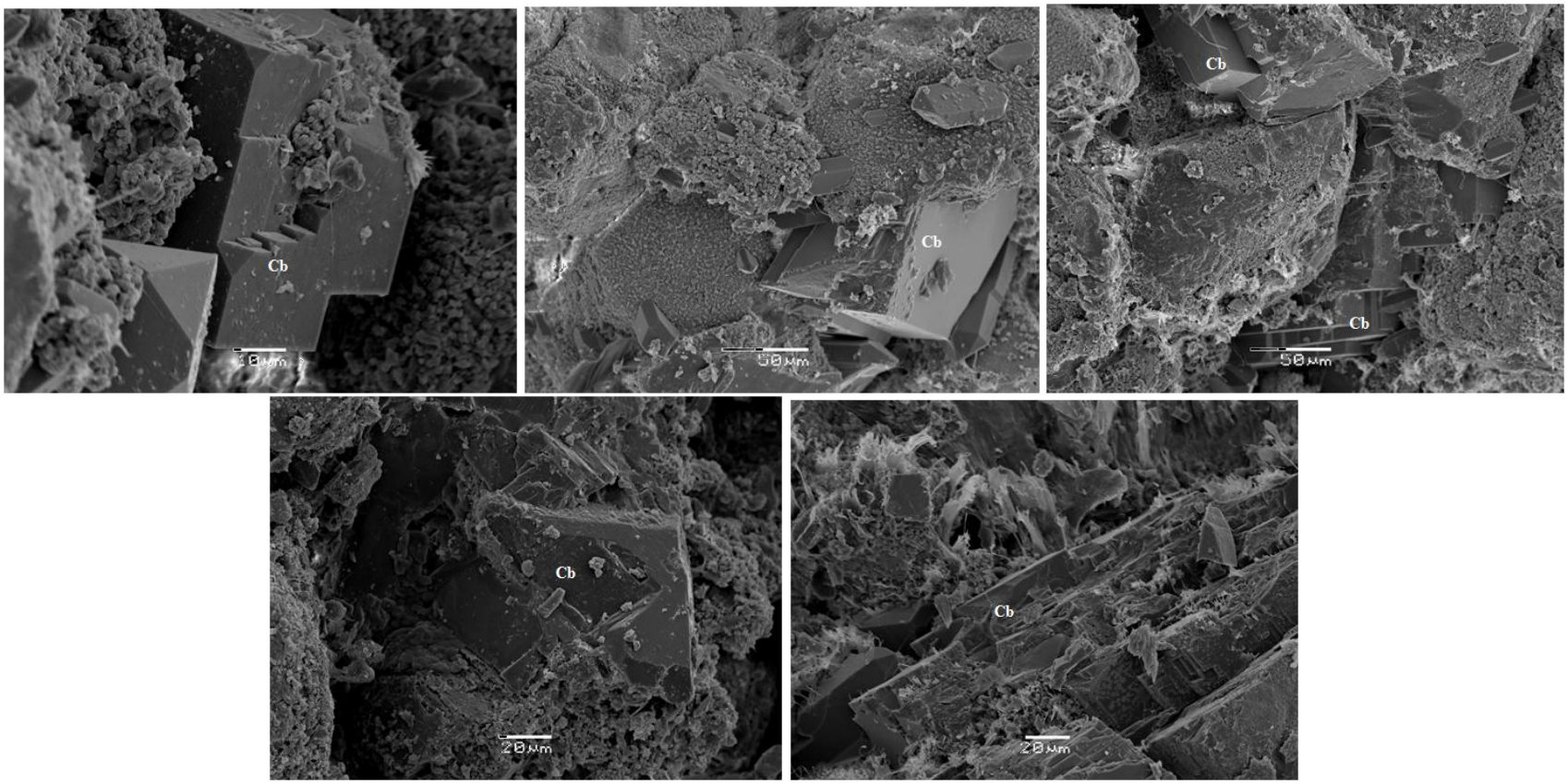
Cb
10μm
Cb
50μm
Cb
Cb
50μm
Cb
20μm
Cb
20μm